University of Alberta

UNITARY AND DIFFERENTIAL UNITARY SPACE TIME MODULATION

by

Mahdi Hajiaghayi

A thesis submitted to the Faculty of Graduate Studies and Research in partial fulfillment of the requirements for the degree of **Master of Science**.

Department of Electrical and Computer Engineering

Edmonton, Alberta
Fall 2007

Library and Archives Canada

Published Heritage Branch

395 Wellington Street
Ottawa ON K1A 0N4
Canada

Bibliothèque et Archives Canada

Direction du Patrimoine de l'édition

395, rue Wellington
Ottawa ON K1A 0N4
Canada

Your file Votre référence
ISBN: 978-0-494-33250-4
Our file Notre référence
ISBN: 978-0-494-33250-4

NOTICE:
The author has granted a non-exclusive license allowing Library and Archives Canada to reproduce, publish, archive, preserve, conserve, communicate to the public by telecommunication or on the Internet, loan, distribute and sell theses worldwide, for commercial or non-commercial purposes, in microform, paper, electronic and/or any other formats.

The author retains copyright ownership and moral rights in this thesis. Neither the thesis nor substantial extracts from it may be printed or otherwise reproduced without the author's permission.

AVIS:
L'auteur a accordé une licence non exclusive permettant à la Bibliothèque et Archives Canada de reproduire, publier, archiver, sauvegarder, conserver, transmettre au public par télécommunication ou par l'Internet, prêter, distribuer et vendre des thèses partout dans le monde, à des fins commerciales ou autres, sur support microforme, papier, électronique et/ou autres formats.

L'auteur conserve la propriété du droit d'auteur et des droits moraux qui protège cette thèse. Ni la thèse ni des extraits substantiels de celle-ci ne doivent être imprimés ou autrement reproduits sans son autorisation.

In compliance with the Canadian Privacy Act some supporting forms may have been removed from this thesis.

While these forms may be included in the document page count, their removal does not represent any loss of content from the thesis.

Conformément à la loi canadienne sur la protection de la vie privée, quelques formulaires secondaires ont été enlevés de cette thèse.

Bien que ces formulaires aient inclus dans la pagination, il n'y aura aucun contenu manquant.

Canada

To my family
You are my everything.

Abstract

Multiple-Input Multiple-Output (MIMO) systems with appropriate space-time (ST) codes can significantly improve the signal transmission's reliability and data rate without power or bandwidth increase. Most ST codes have been designed by assuming that the receiver knows the channel state information (CSI). However, obtaining up-to-date and accurate CSI is not always possible, especially in fast-fading MIMO channels. In this case, unitary space-time modulation (USTM) and differential USTM (DUSTM) can be employed to exploit the benefits of the MIMO. These techniques require a fixed codebook of unitary matrices known a priori to both the receiver and transmitter. The design measure and optimum codebook, which may vary with the MIMO system characteristics, are of interest in this dissertation which introduces two new unitary constellations and proposes a general design criterion applicable to any MIMO characteristic. Genetic-algorithm search and exhaustive search are used to find the optimum codebooks since analytic solutions are intractable. The performance of the Maximum Likelihood (ML) and Non-ML receivers is investigated for all types of MIMO channels. Due to the benefits of antenna selection in terms of reducing the number of RF chains, the performance of the USTM with antenna selection over a correlated Rayleigh channel is studied. The influence of the correlation coefficient and Ricean K-factor on the system bit error rate (BER) performance is quantified.

Acknowledgements

During my M.Sc study, I met many exceptional individuals. I would like to express my deep gratitude to my supervisor, Professor Chintha Tellambura, for his constant support throughout this work. His door was always open whenever I ran into a problem or had a question about anything.

I am deeply grateful to the members of my committee, Dr. Ardakani and Dr. Gburzynski, for their time and advice.

My special thanks goes to my former and current roommates, Dr. Ramin Sarrami and Matlock Bolton, who besides providing me with a friendly environment full of humor and joy, also enriched my knowledge of Medicine, Biology, the English language and life in general. I was so lucky to live with them.

I would like to thank my colleagues at the *i*CORE Wireless Lab, Alireza Ghaderipour, Saeed Kaviani, Raman Yazdani, Ali Sanaei, Khoa T. Phan and Tyler Nechiporenko, for their valuable hints, extensive discussions and support helped me to finish this thesis. Without their help, completing my thesis would have been impossible.

Last but not least, my deepest gratitude goes to my parents and my brother, Dr. MohammadTaghi. I have benefited from their help and guidance throughout my life. As well, I thank my sisters, Monir and Mehri, for their encouragement and loving support. Although they are living far from here, their warm and endless support in many ways enabled me to complete my thesis.

Table of Contents

1 Introduction 1
- 1.1 Motivation . . . 1
- 1.2 Contributions . . . 3
- 1.3 Thesis Outline . . . 4

2 Preliminaries and Background 5
- 2.1 Space Time Code, Spatial rate and Diversity . . . 5
- 2.2 MIMO Systems . . . 6
  - 2.2.1 MIMO System Model . . . 6
  - 2.2.2 Maximum Likelihood (ML) Detection . . . 7
  - 2.2.3 ST Code Design . . . 7
- 2.3 Communication Channel Models . . . 9
  - 2.3.1 Spatially fading correlation . . . 9
  - 2.3.2 Ricean Channel . . . 10
- 2.4 USTM and DUSTM . . . 11
  - 2.4.1 USTM . . . 11
  - 2.4.2 DUSTM . . . 12
- 2.5 Antenna Selection . . . 13
  - 2.5.1 Maximizing information rate criterion . . . 14
  - 2.5.2 Minimizing Error rate approach . . . 15
- 2.6 Decoding Techniques . . . 16
- 2.7 Summary . . . 17

3 Differential Unitary Space-Time Code design 18
- 3.1 Introduction . . . 18
- 3.2 Code Design Criteria and Approximate Union Bound . . . 19
- 3.3 Unitary Constellation Design . . . 20
- 3.4 Exhaustive Computer Search . . . 22
  - 3.4.1 Simulation Results and Discussion . . . 24
- 3.5 Genetic Algorithm Search method . . . 25
  - 3.5.1 Genetic Algorithms . . . 26
  - 3.5.2 Simulation Results and Discussion . . . 29
- 3.6 Summary . . . 29

4 Optimum Design DUSTM for Transmit-Correlated Channel 31
- 4.1 Introduction . . . 31
- 4.2 DUSTM over Transmit Correlation . . . 32
  - 4.2.1 Pairwise Error Probability in case of DUST Code . . . 33
- 4.3 Code Design . . . 33
- 4.4 Simulation Results . . . 36
- 4.5 Summary . . . 38

5 Antenna Selection for USTM over Correlated and Ricean Channels **39**
5.1 Introduction 39
5.2 System Model and USTM Scheme 40
5.3 Error Probability of USTM RAS in Correlated Fading 41
5.3.1 Exponential Correlation Case 43
5.3.2 Constant Correlation Case 47
5.4 Extension to Ricean-Fading Channels 50
5.4.1 Chernoff Bound and Performance Analysis 51
5.5 Simulation Results 56
5.6 Summary 57

6 Conclusion and Future Research **60**

A Appendices **62**
A.1 Proof of Theorem 5.3.2 62
A.2 Proof of Theorem 5.3.2 62
A.3 Demonstration of Convergence Properties of Proposed Series and [1] 63

List of Figures

1.1 A MIMO wireless system with multiple TX and RX antennas. . . . 2
1.2 Capacity (in normalized Shannon capacity) vs. $r = \min(M, N)$ for 0dB $< \rho <$ 35dB in 5dB increments, Source: [3] 2

2.1 Transmit/Receive antenna switching schematic 14

3.1 Symbol Error Rate of two different constellation with $M = 3$, $N = 2$ for Differential receiver. 25
3.2 one-point crossover technique 27
3.3 two-points crossover technique 27
3.4 Symbol Error Rate performance of cyclic and cyclic rotated design when $L = 16$, $M = 6$ and $N = 1$. The dashed line curves are for exhaustive search and solid lines are for genetic search. 30

4.1 Symbol Error Rate of two different constellation with $M = 3$, $N = 1$ for ML receiver and Non-ML(Differential) receiver. 37
4.2 Performance comparison of ML and Non-ML receivers on the optimum code in constellation (2.3.1) when $M = 2$, $N = 2$ and $L = 8$. 38

5.1 Comparison of the approximation and exact curve of $F_z(a)$ assuming constant correlation matrix with $\gamma = 0.5$ 50
5.2 Comparison of the Chernoff bound and the simulated PEP with $M = 2, N = 2\ J = 1$ 57
5.3 Performance comparison of parametric codes for the system with or without antenna selection and $M = 2$, $L = 16$ over spatially correlated channel 58
5.4 Comparison of the Chernoff bound and the simulated PEP for different K-factor $M = 2, N = 2\ J = 1$ 59
5.5 Performance comparison of parametric codes for the system with or without antenna selection and M=2, L=16 over a Ricean channel K=2 59

A.1 Comparison of the convergence properties of the power series expansion and our formula for $F_z(a)$ assuming constant correlation matrix with $\gamma = 0.5$ 66

List of Notations

$\min(a, b)$	Minimum value of a and b
$\otimes$	Kronecker matrix product
$(\cdot)^T$	Matrix transpose
$(\cdot)^H$	Conjugate transpose of the matrix argument
$\Re\{\cdot\}$	Real part of the matrix argument
$\Im\{\cdot\}$	Imaginary part of the matrix argument
$E\{\cdot\}$	Expectation operation
$\mathbf{A}$	the Matrix $\mathbf{A}$
$\mathbf{a}$	the vector $\mathbf{a}$
$\mathbf{A}(k, :)$	The k^{th} row of the matrix $\mathbf{A}$
$\det\{\mathbf{A}\}$	Determinant of the matrix $\mathbf{A}$
$\|\mathbf{A}\|$	Frobenius norm of the matrix $\mathbf{A}$
$r(\mathbf{A})$	Rank of the matrix $\mathbf{A}$
$\mathcal{CN}(\mu, \sigma^2)$	A circularly symmetric complex Gaussian random variable (RV) with mean μ and variance σ^2

Abbreviations

ADC	analog to digital converter
AWGN	additive white Gaussian noise
BER	bit error rate
BPSK	binary pulse shift keying
CSI	channel-side information
cdf	cumulative density function
DUSTM	differential unitary space time modulation
i.i.d	independent and identically distributed
GA	genetic algorithm
LOS	line of sight
MGF	moment generating function
MIMO	multiple-input multiple-output
ML	maximum likelihood
MMSE	minimum mean square error
OSTBC	orthogonal space-time block code
PAM	pulse amplitude modulation
pdf	probability density function
PSK	pulse shift keying
QAM	quadrature amplitude modulation
RF	radio frequency
RV	random variable
SER	symbol error rate
SISO	single input single output
SNR	signal to noise ratio
ST	space time
STBC	space-time block code
USTM	unitary Space Time Modulation
V-BLAST	vertical bell laboratories layered space-time
ZF	zero-forcing

Chapter 1

Introduction

1.1 Motivation

Wireless networks and devices are ubiquitous and the ultimate goal of wireless communication is to facilitate any-place any-time communications. To achieve this desired goal, future wireless systems must provide higher bandwidth efficiency and data rates. This requirement is particularly challenging for systems that are power, bandwidth and complexity limited.

In 1999, the use of multiple transmit and/or receive antenna was proposed and shown to be very effective in reaching to the upper bound of the achievable data rate (Shanon capacity). Previously, wireless engineers treated multipath propagation as a problem to be mitigated whereas MIMO wireless technology exploits multipath propagation to improve the quality of service measures such as the bit error rate (BER) or the data rate (bits/sec). In other words, MIMO effectively takes advantage of random fading and multipath delay spread to increase the data transfer rate [5].

Exploiting the benefits of MIMO channels requires the use of Space-Time (ST) codes. The ST code design, a major challenge in MIMO systems, involves finding an optimal way of encoding and transmitting multiple copies of a data stream across multiple antennas to improve the rate and reliability of data transfer.

Fig. 1.1 shows a MIMO system model. A binary data stream after traditional operations such as error-control coding and interleaving are mapped to complex modulation symbols (for instance, quaternary phase-shift keying [QPSK]), and these symbols are transmitted over multiple antennas. The receiver captures the

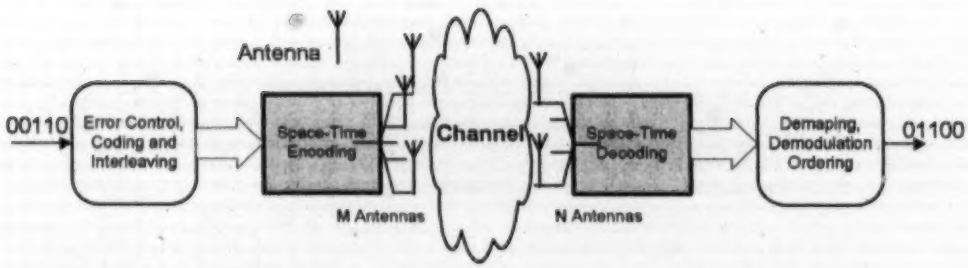

Figure 1.1: A MIMO wireless system with multiple TX and RX antennas.

multiple received antenna signals and extracts the transmitted data by using ST decoding techniques.

The theoretical analysis in [5] shows that the capacity of a MIMO system increases linearly with the minimum number of transmitter and receiver antennas. Fig. 1.2 depicts how the capacity of a MIMO system varies with a minimum of M transmit and N receive antennas for different values of SNR(ρ).

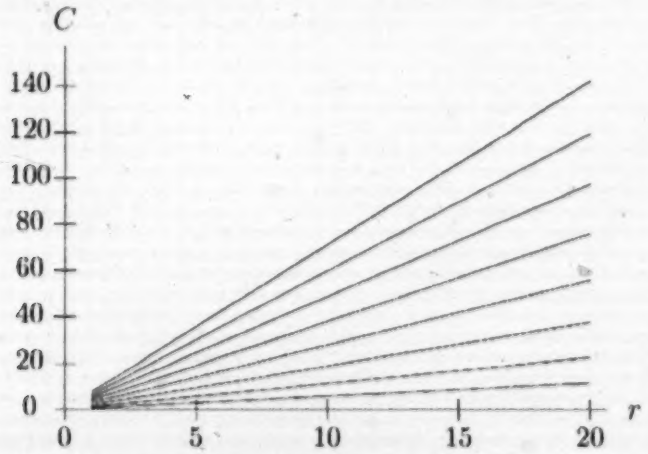

Figure 1.2: Capacity (in normalized Shannon capacity) vs. $r = \min(M, N)$ for 0dB $< \rho <$ 35dB in 5dB increments, Source: [3]

The initial work on ST code design has studied the case where the receiver knows the channel state information (CSI) between each transmit and receive antenna. If an accurate and up-to-date CSI is not available, unitary space time modulation(USTM) and differential USTM (DUSTM) [introduced by Hochwald et. al in [6] and [7]] can be employed to exploit the benefits of the MIMO systems' prop-

erties.

1.2 Contributions

In this thesis, we provide a coherent analysis of USTM and DUSTM and examine their performance with respect to the data rate and error probability under different practical assumptions. The contributions of this thesis can be divided into three main parts:

- A new structure of unitary matrices is introduced, and the optimal codebook of DUSTM is searched based on minimizing union bound for the case of the Rayleigh fading channel. A good and easy-to-compute approximation of union bound on symbol error probability is derived that can be applied to any unitary constellation of any size. By introducing a genetic algorithm (GA), the design parameters, which used to be integers in the case of an exhaustive search, can be relaxed to real parameters. The simulation results show that this relaxation result in a better performance.

- The performance analysis of a MIMO system employing differential USTM is carried out under the assumption of a spatially correlate-fading channel, and a design criterion to construct the differential codebook of unitary matrices is presented. Based on minimizing union bound, we search for the optimum constellation parameters. In simulation section, the performances of the ML and and Non-ML decoders for this case are investigated.

- Antenna selection and USTM are extended into correlated Rayleigh or Ricean fading channels. Antenna selection in the USTM case is performed based on the maximum norm criterion. The Chernoff bound on PEP is derived for the selection of a single antenna. The analytical results as well as simulation results indicate that the full diversity is preserved for both correlated and Ricean channels. However, in the correlated channel case, there is a loss in the coding gain.

1.3 Thesis Outline

This thesis is organized as follows:

- Chapter 2 briefly reviews different mathematical models of a MIMO system and introduces some required concepts in MIMO such as diversity, pairwise error probability, ST code design and antenna selection.

- Chapter 3 introduces the two new constellations of unitary matrices and presents an accurate and easy-to-compute approximation of union bound on the symbol error probability (SEP) as the ST design criterion. By using an exhaustive search and a genetic search, the optimum codes with integer and real parameters are found, and their performance are examined and compared through the simulations.

- In Chapter 4, the DUSTM design criterion under the assumption of a transmit correlated-fading channel is presented. Considering the unitary matrix constellations introduced in Chapter

  3, we search for the constellation parameters to minimize the union bound on SEP by taking into account the number of receive and transmit antenna.

- Chapter 5 investigates the performance of the USTM by employing single antennas selection in the non-independent fading channels. The Chernoff bound on the PEP is derived for the case selecting the 'best' single antenna, and the diversity order and coding gain are obtained for the both correlated and Ricean channel cases.

Chapter 2

Preliminaries and Background

This chapter provides a general introduction to multiple-input multiple-output (MIMO) systems and space time coding. Important MIMO concepts and definitions, such as space time (ST) codes, spatial rate, diversity order and coding gain, are presented in Section 2.1. The MIMO system model, design criteria and ST codes are discussed in Section 2.2.1. MIMO channel models are described in Section 2.3. Unitary space time modulation (USTM) and differential unitary space time modulation (DUSTM) schemes are briefly reviewed in Section 2.4. Antenna selection techniques along with different decoding techniques are presented in Sections 2.5 and 2.6, respectively.

2.1 Space Time Code, Spatial rate and Diversity

The general structure of an ST code can be represented by an $M \times T$ matrix:

$$\mathbf{S} = \begin{bmatrix} s_{1,1} & \cdots & s_{1,T} \\ \vdots & \ddots & \\ s_{M,1} & \vdots & s_{M,T} \end{bmatrix}, \tag{2.1}$$

where $s_{i,j}$ is the modulation symbol transmitted in time slot j from antenna i, T is the number of time slots, and M is the number of transmit antennas. Each column represents a time slot, and each row stands for one antennas's transmissions over T time slots. The number of independent symbols in $\mathbf{S}$ divided by T is called the *spatial rate*.

In wireless channels, the probability of signal fading decreases when the number of independent antenna elements is increased. The diversity order relates to

the number of uncorrelated spatial branches available at the transmitter or receiver. The diversity order is mathematically defined as follows: at asymptotically high signal-to-noise ratio (SNR) denoted by ρ, if the symbol error rate (SER) P_e can be approximated as

$$P_e \approx (G_c \rho)^{-G_d}, \tag{2.2}$$

then G_c and G_d represent the diversity order and *diversity gain*, respectively. That is, the diversity order is defined as the magnitude of the slope of the SER vs. the SNR graph on a log-log scale. MIMO systems should be designed to achieve the maximum diversity order. Since the diversity order of a MIMO system depends on the type of coding and modulation scheme as well as the number of transmit and receive antennas, diversity issues have been widely investigated [8], [1]. Besides improving error performance by maximizing the diversity order, the coding gain, which depends on the minimum distance of the ST code, should also be improved.

In the literature, a variety of ST coding schemes support different tradeoffs between rate, diversity order and coding/array gain. The details of ST code designs and MIMO model are described next.

2.2 MIMO Systems

2.2.1 MIMO System Model

Consider a MIMO system with M transmit and N receive antennas operating over a frequency-flat channel that remains constant for at least T signaling intervals. From (2.1), the information bit stream is encoded into a ST codeword of dimension $T \times M$. The ST codeword is defined by $\mathbf{S} = [\mathbf{s}_1, \mathbf{s}_2, \ldots, \mathbf{s}_T]^T$, where $\mathbf{s}_t$ is the transmitted vector symbol over the tth time slot. In this time slot, the complex symbols $s_{t,i}$ are transmitted over antennas $i = 1, \ldots, M$, and $y_{t,j}$ is received on receiver antennas $j = 1, \ldots, N$. As well, $h_{i,j}$ is denoted as the fading coefficient from the ith transmit antenna to the jth receive antenna. The input-output relation is given by

$$y_{t,j} = \sqrt{\frac{\rho}{M}} \sum_{i=1}^{M} h_{i,j} s_{t,i} + w_{t,j} \quad t = 1, \ldots, T, j = 1, \ldots, N, \tag{2.3}$$

where the additive noise at time t in the receive antenna j denoted by $v_{t,j}$ is independently, identically distributed (i.i.d.) $\mathcal{CN}(0,1)$. The average signal-to-noise ratio (SNR) per receive antenna is ρ. Eq. (2.3) can be written in a matrix form as

$$\mathbf{Y}_t = \sqrt{\frac{\rho}{M}}\mathbf{S}_t\mathbf{H}_t + \mathbf{W}_t, \tag{2.4}$$

where $\mathbf{Y}_t$ is the $T \times N$ complex received signal matrix, and $\mathbf{S}_t$ is the $T \times M$ complex transmitted signal matrix at the time index t. $\mathbf{H}_t$ is the $M \times N$ channel transfer function, and $\mathbf{W}_t$ denotes a $T \times N$ additive noise matrix with i.i.d. $\mathcal{CN}(0,1)$ elements.

2.2.2 Maximum Likelihood (ML) Detection

Different detection techniques are available to recover the transmitted data. In Maximum Likelihood (ML) detection, the receiver uses perfect CSI to estimate the transmitted signal matrix. The ML detection rule can be expressed as

$$\mathbf{S}_{ML} = \arg\min_{\mathbf{S}} \|\mathbf{Y}_t - \sqrt{\frac{\rho}{M}}\mathbf{S}\mathbf{H}_t\|_F^2 = \arg\min_{\mathbf{S}} \sum_{t=1}^{T} \|\mathbf{y}_t - \sqrt{\frac{\rho}{M}}\mathbf{s}_t\mathbf{H}_t\|_F^2 \tag{2.5}$$

where the minimization is performed over all admissible codewords $\mathbf{S}$. An error occurs when the detector output (2.5) is not the same as the transmitted matrix. In this case, the receiver mistakes a transmitted codeword for another codeword from the set of possible codewords.

2.2.3 ST Code Design

ST code design is an active area of research in MIMO systems. Design may depend on many parameters such as the signaling scheme, the availability of the CSI at the receiver, the rate of data transmission and the method of detection. However, a general formula to derive ST code design criteria has been proposed by Tarokh et al. in [9]. They showed that in the high SNR regime ($\rho >> 1$), the upper bound on pairwise error probability of mistaking transmitted codeword $\mathbf{S}_i$ for another codeword $\mathbf{S}_j$ is expressed as

$$P(\mathbf{S}_i \rightarrow \mathbf{S}_j) \leq \frac{1}{\det(\mathbf{G}_{i,j})} \left(\frac{\rho}{4M}\right)^{-\mathbf{r}(\mathbf{G}_{i,j})N}, \tag{2.6}$$

where $\mathbf{G}_{i,j} = (\mathbf{S}_i - \mathbf{S}_j)(\mathbf{S}_i - \mathbf{S}_j)^H$. From (2.6), two important criteria can be derived for ST code construction. First, the *rank criterion* aims to maximize the diversity order, i.e. to maximize $r(\mathbf{G}_{i,j})N$. Hence, to extract the maximum diversity, one should maximize the minimum rank of the difference matrix between any pair of codewords $\mathbf{S}_i$ and $\mathbf{S}_j$ and possibly make it full rank ($r(\mathbf{G}_{i,j}) = M$) by designing a proper ST codebook . Second, the *determinant criterion* deals with the optimization of the coding gain for the ST code. To obtain a high coding gain, one should maximize the minimum of the determinant of $\mathbf{G}_{i,j}$ over all possible codewords $\mathbf{S}_i$ and $\mathbf{S}_j$. Both these criteria lead ultimately to the minimization of the error probability.

In the literature, a variety of ST codes support different tradeoffs among the rate, diversity order and coding gain. Orthogonal space time block code (OSTBC) is one of the well-known classes of ST codes with spatial rate $r_s \leq 1$ because it not only provides a full diversity order, but also leads to very simple and low-complexity ML receiver. OSTBC's are based on orthogonal design. A simple form of OSTBC is the Alamouti code with spacial rate $r_s = 1$, which can be expressed as [10]

$$\mathbf{S} = \begin{bmatrix} s_1 & -s_2^* \\ s_2 & s_1^* \end{bmatrix}. \tag{2.7}$$

The codeword difference matrix between any pair of codewords $\mathbf{S}_i$ and $\mathbf{S}_j$ in this case is an orthogonal matrix with two non-zero eigenvalues, leading to full $2N$ order diversity. Due to the orthogonal structure of OSTBC's, the complex vector ML detection problem in (2.5) decouples into a set of simpler scalar detection problems with significantly less computational complexity. A question may arise: Whether an Orthogonal ST code necessarily exists for any number of transmit antennas with spatial rate 1? In fact, it has been shown at least one orthogonal ST codeword can be found to transmit real symbols for a system with any number of transmit antenna [11]. For instance, one orthogonal design for $M = 4$ with spatial rate 1 is given by

$$\mathbf{S} = \begin{bmatrix} s_1 & -s_2 & -s_3 & -s_4 \\ s_2 & s_1 & s_4 & -s_3 \\ s_3 & -s_4 & s_1 & s_2 \\ s_4 & s_3 & -s_2 & s_1 \end{bmatrix}, \tag{2.8}$$

where symbols s_1, s_2, s_3 and s_4 are drawn from a real constellation. In the complex-symbol case, it has been proved that no orthogonal ST code exists with spatial rate

1 for systems with more than two transmit antenna [9]. However, it has been shown that at least one orthogonal design exists for rates equal or less than $\frac{1}{2}$ [11]. For instance, when $M = 3$, a rate $\frac{1}{2}$ orthogonal design is:

$$\mathbf{S} = \begin{bmatrix} s_1 & -s_2 & -s_3 & -s_4 & s_1^* & -s_2^* & -s_3^* & -s_4^* \\ s_2 & s_1 & s_4 & -s_3 & s_2^* & s_1^* & s_4^* & -s_3^* \\ s_3 & -s_4 & s_1 & s_2 & s_3^* & -s_4^* & s_1^* & s_2^* \end{bmatrix}. \tag{2.9}$$

So far, ST codes with spatial rate $r_s \leq 1$ with full diversity order MN have been discussed. Notice that in order to decode this class of ST codes, the CSI is required by the receiver. We will later consider USTM that enables the decoding without having CSI at the receiver. Different types of wireless channel models are described next.

2.3 Communication Channel Models

In the classical Rayleigh fading channel, all entries of channel matrix $\mathbf{H}$ in (2.4) are assumed to be i.i.d. complex Gaussian RV $\mathcal{CN}(0, 1)$. In reality, however, insufficient antenna spacing, angle spread or the lack of rich scattering may cause spatial correlation among antennas, particularly at the transmit side [12](because the transmitter usually has more antennas than the receiver). Moreover, channel measurements reveal that propagation environment have a fixed [possibly line of sight(LoS)] component. Those cases are modeled as the Ricean channel, in which the mean of the elements in the channel matrix model is not zero. In the following, we present the mathematical models of spatially correlated and Ricean channels.

2.3.1 Spatially fading correlation

The effects of spatial fading correlation for a Rayleigh flat fading channel can be modeled as

$$\mathbf{H} = \mathbf{R}_T^{1/2} \mathbf{H}_w \mathbf{R}_R^{1/2}, \tag{2.10}$$

where the matrices $\mathbf{R}_T$ and $\mathbf{R}_R$ denote the transmit and receive correlation matrices, respectively. $\mathbf{R}_T$ and $\mathbf{R}_R$, which are positive-definite Hermitian matrices, are normalized so that $[\mathbf{R}_T]_{i,i} = 1 (i = 1, \cdots, M)$, and $[\mathbf{R}_R]_{i,i} = 1 \quad (i = 1, \cdots, N)$,

resulting in $E\{|h_{i,j}|^2\} = 1$. $\mathbf{H}_w$ is the $M \times N$ matrix with i.i.d. $\mathcal{CN}(0,1)$ RVs entries.

Several transmit/receive correlation models are available in the literature. The first model is the *exponential correlation* model [13]. This model may hold for the practical case of the equispaced linear array of antennas. The correlation matrix and corresponding eigenvalues of this model are given by [13]

$$\mathbf{R}_T = \begin{bmatrix} 1 & \gamma & \cdots & \gamma^{M-1} \\ \gamma & 1 & \cdots & \gamma^{M-2} \\ \vdots & \vdots & \ddots & \vdots \\ \gamma^{M-1} & \gamma^{M-2} & \cdots & 1 \end{bmatrix} \tag{2.11}$$

and

$$\lambda_i = \frac{1-\gamma^2}{1-2\gamma\cos(\theta_i)+\gamma^2} \quad i = 1, 2, \ldots, M,$$

where θ_i are the values of θ which satisfy one or the other of the equations:

$$\begin{cases} \sin(\frac{M+1}{2}\theta) = \gamma\sin(\frac{M-1}{2}\theta), \\ \cos(\frac{M+1}{2}\theta) = \gamma\cos(\frac{M-1}{2}\theta). \end{cases}$$

The *constant correlation* matrix is another practical model frequently used for an array of three antennas placed on an equilateral triangle or closely spaced antennas [14]. The correlation matrix in this case is written as

$$\mathbf{R}_T = \begin{bmatrix} 1 & \gamma & \cdots & \gamma \\ \gamma & 1 & \cdots & \gamma \\ \vdots & \vdots & \ddots & \vdots \\ \gamma & \gamma & \cdots & 1 \end{bmatrix}. \tag{2.12}$$

In this case, $\mathbf{R}_T$ has only two eigenvalues $\lambda_1 = 1 + \gamma(M-1)$ of order one and $\lambda_2 = 1 - \gamma$ of order $M - 1$.

Similarly, these models can also be applied to model the receive correlation matrix. The correlation matrices have a degradation effect on the capacity of the MIMO channel [15]. This issue is explored in Chapter 4.

2.3.2 Ricean Channel

The $M \times N$ random channel matrix $\mathbf{H}$ in this case is decomposed into the sum of a fixed component and a variable component. The channel realization would be

$$\mathbf{H} = \sqrt{\frac{K}{K+1}}\overline{\mathbf{H}} + \sqrt{\frac{1}{K+1}}\mathbf{H}_w, \tag{2.13}$$

where the first and second term in (2.13) represent the mean value (called the line of sight component) and the variable part (called the diffuse component) of the communication channel, respectively. The Ricean factor K measures the relative strength of the LOS component, a link-quality indicator ([16]). The elements of $\mathbf{H}_w$ are i.i.d. complex Gaussian random variables, i.e., $\mathcal{CN}(0,1)$. $K = 0$ corresponds to the pure Rayleigh fading case while $K = \infty$ indicates a non-fading channel. As an example for a typical matrix of $\overline{\mathbf{H}}$, we can use the following matrices for a MIMO channel with $M = N = 2$ [11]:

$$\overline{\mathbf{H}}_1 = \begin{bmatrix} e^{j\theta_1} & 0 \\ 0 & e^{j\theta_2} \end{bmatrix} \begin{bmatrix} 1 & 1 \\ 1 & 1 \end{bmatrix} \begin{bmatrix} e^{j\theta_3} & 0 \\ 0 & e^{j\theta_4} \end{bmatrix}$$

$$\overline{\mathbf{H}}_2 = \begin{bmatrix} e^{j\theta_1} & 0 \\ 0 & e^{j\theta_2} \end{bmatrix} \begin{bmatrix} 1 & -1 \\ 1 & 1 \end{bmatrix} \begin{bmatrix} e^{j\theta_3} & 0 \\ 0 & e^{j\theta_4} \end{bmatrix}, \tag{2.14}$$

where θ_i's are phase factors determined by the array geometry model and orientation. Note that the fixed component of the channel matrix plays a critical role in channel capacity at a high K-factor. For instance, at an SNR of 10dB and $K = 20$, the outage capacity of $\overline{\mathbf{H}}_2$ is almost twice the outage capacity of $\overline{\mathbf{H}}_1$ due to the orthogonal property of $\overline{\mathbf{H}}_2$. The Ricean channel is treated in Chapter 5

2.4 USTM and DUSTM

As mentioned before, USTM is an important technique for transmitting data and achieving capacity in a MIMO system at high SNR when the CSI is unavailable. This technique can be seen as a multiple antenna extension of phase-shift keying (PSK) for scalar channels. Similarly, the differential USTM is also a generalization of differential PSK in a MIMO system [17], [6]. The rest of this section explains exactly how this modulation technique operates and examines its performance in terms of the pairwise error probability (PEP) and data rate.

2.4.1 USTM

Assume that a data sequence of integers $d_1, d_2, \ldots$ with $d_t \in \{0, \ldots, L-1\}$ is to be transmitted. Each d_t is mapped to a matrix Φ_{d_t} drawn from a codebook, say

$\mathcal{V} = \{\mathbf{\Phi}_l | l = 0, \ldots, L-1\}$, where each $T \times M$ matrix $\mathbf{\Phi}_l$ satisfies $\mathbf{\Phi}_l^H \mathbf{\Phi}_l = I_M$ (unitary property). The positive integer $L \geq 2$, which denotes the constellation size, should be $L = 2^{RM}$ in order to reach to the data rate R [bits/channel]. In the USTM scheme, to send data d_{z_t}, the associated transmitted signal $\mathbf{S}_t = \sqrt{T}\mathbf{\Phi}_{z_t}$ is transmitted over multiple antennas. The scaling factor $\sqrt{T}$ ensures that the signals satisfy the energy constraint.

We consider the ML reception of this scheme, and its performance is presented when H is unknown to the receiver. Due to the unitary property of the transmitted signal, the received signal is complex Gaussian. As a result, conditioned on $\mathbf{S}_l$, the conditional probability density of $\mathbf{Y}$ is obtained as [6]

$$p(\mathbf{Y}|\mathbf{S}_l) = \frac{\exp\left(-\operatorname{tr}[\mathbf{Y}\mathbf{R}_l^{-1}\mathbf{Y}]\right)}{\pi^{TN}\det(\mathbf{R}_l)}, \tag{2.15}$$

where $\mathbf{R}_l = (\rho T/M)\mathbf{\Phi}_l\mathbf{\Phi}_l^H$ is the $T \times T$ received covariance matrix. According to [6], by using matrix inversion lemma and showing that the denominator of (2.15) is independent of $\mathbf{\Phi}_l$, the ML decoding rule becomes

$$\mathbf{\Phi}_{ml} = \arg\max_{\phi_l \in \mathcal{V}} p(\mathbf{Y}|\mathbf{\Phi}_l) = \arg\max_{\phi_l \in \mathcal{V}} \operatorname{tr}\{\mathbf{Y}^H \Phi_l \mathbf{\Phi}_l^H \mathbf{Y}\}. \tag{2.16}$$

Since the receiver is aware of the codebook $\mathcal{V}$, it performs ML detection of (2.16) over all unitary matrices Φ_l and extracts the most likely transmitted signal. Note that in (2.16), no CSI is needed to detect the transmitted matrix. Assuming a Rayleigh fading channel remains constant during T consecutive symbol periods, the PEP of mistaking $\mathbf{\Phi}_{l'}$ for $\mathbf{\Phi}_l$ or vice versa is derived in [6]

$$P_{l,l'} = \frac{1}{4\pi}\int_{\infty}^{\infty} d\omega \frac{1}{\omega^2 + 1/4} \times \prod_{m=1}^{M}\left[1 + \frac{(\rho T/M)^2(1-d_{llm}^2)(\omega^2+1/4)}{1+\rho T/M}\right]^{-M} \tag{2.17}$$

where $1 \geq d_{ll'1} \geq \cdots \geq d_{ll'M} \geq 0$ are the singular value of the $M \times M$ correlation matrix $\mathbf{\Phi}_l^H \mathbf{\Phi}_{l'}$. Further results for USTM will be presented later.

2.4.2 DUSTM

In DUSTM [2], d_{z_t} is mapped to an $M \times M$ distinct unitary matrix $\mathbf{\Phi}_{z_t}$. As a result, the transmitted signal $\mathbf{S}_t$ at time t is given by

$$\mathbf{S}_t = \begin{cases} \mathbf{\Phi}_{z_t}\mathbf{S}_{t-1} & t = 1, 2 \ldots, \\ \mathbf{I}_M & t = 0. \end{cases} \tag{2.18}$$

We combine two consecutive received signal matrices by using (2.18) and (2.3) and assume that the channel coefficients are almost constant for two signaling blocks; i.e., $\mathbf{H}_t \simeq \mathbf{H}_{t-1}$. As a result, the fundamental differential system relation is given by

$$\mathbf{Y}_t = \mathbf{\Phi}_{z_t}\mathbf{Y}_{t-1} + \sqrt{2}\mathbf{W}'_t, \tag{2.19}$$

where $\mathbf{W}'_t = (1/\sqrt{2})(\mathbf{W}_t - \mathbf{\Phi}_{z_t}\mathbf{W}_{t-1})$ is an $M \times N$ additive independent noise matrix with $\mathcal{CN}(0,1)$. It is shown in [6] that the ML detection rule would be

$$\widehat{d}_t = \arg\min \|\mathbf{Y}_t - \mathbf{\Phi}_l\mathbf{Y}_{t-1}\|, \tag{2.20}$$

and the exact PEP for a Rayleigh fading channel may be expressed as

$$P_{ll'} = p(\mathbf{\Phi}_l \longrightarrow \mathbf{\Phi}_{l'}) = \frac{1}{\pi}\int_0^{\frac{\pi}{2}} \prod_{i=1}^{M} (1 + \frac{\gamma\lambda_i}{4\sin(\theta)^2})^{-N} d\theta \tag{2.21}$$

where $\gamma = \frac{\rho^2}{1+2\rho}$ and $\{\lambda_i\}$ is the ith eigenvalue of the matrix $\Delta_{ll'} = (\mathbf{\Phi}_l - \mathbf{\Phi}_{l'})(\mathbf{\Phi}_l - \mathbf{\Phi}_{l'})^H$.

As described in [2], the DUSTM scheme can be viewed as a special case of the general USTM scheme by defining an equivalent $T \times M$ unitary matrix $\tilde{\mathbf{\Phi}}_{z_t}$ of the form $\tilde{\mathbf{\Phi}}_{z_t} = 1/\sqrt{2}[\mathbf{I}_M, \mathbf{\Phi}_{z_t}]$. In this case, $T = 2M$.

The antenna selection technique and its performance in a MIMO system will be briefly investigated in the next section.

2.5 Antenna Selection

The main drawback of any MIMO system with M transmit and N receive antennas is the increased complexity and cost since this system requires complete transceiver hardware such as transmit amplifiers and D/A converters for each antenna. A promising strategy that can significantly reduce this complexity and simultaneously keep almost all the benefits of a MIMO system is to select a subset of antennas at the transmitter and/or receiver. This strategy has been considered by many researchers during the past five years, and different criteria and effective algorithms to select the best antennas have been proposed as well [18], [19] and [20].

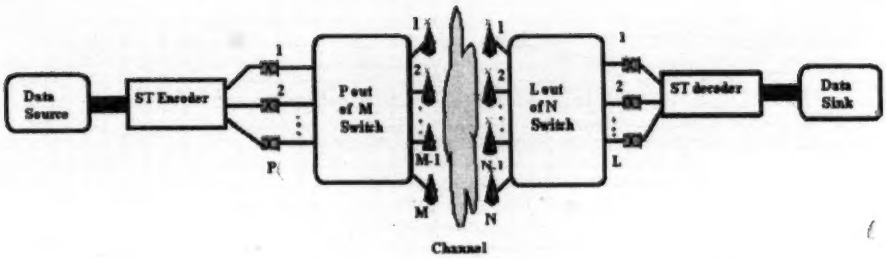

Figure 2.1: Transmit/Receive antenna switching schematic

Fig. 2.1 depicts a system with antenna selection at the transmitter and receivers sides. Assuming we want to choose P transmit and L receive antennas, there are $\binom{M}{P} \times \binom{N}{L}$ distinct sub-channel choices where the channel corresponding to the ith choice is denoted by $\mathbf{H}_i$. T the dimension of $\mathbf{H}_i$ for any i is $P \times L$ comprising the P selected columns and L selected rows of $\mathbf{H}$.

Depending on the signaling schemes and the availability of the CSI at the transmit and receiver sides, several different optimization criteria for antenna selection may be present. However, two main approaches for antenna selection are available: (1) maximizing the mutual information rate (capacity) and (2) minimizing the error rate. A detailed discussion of these criteria is beyond the scope of this thesis. However, a brief explanation is provided here, since they will later be used in Chapter 5.

2.5.1 Maximizing information rate criterion

The capacity (maximum data rate) of a MIMO system employing all antenna elements is given by [3]

$$C = \log_2 \left[\det \left(I_M + \frac{\rho}{M} \mathbf{H}\mathbf{H}^H \right) \right], \tag{2.22}$$

where ρ is the average SNR per receiver. If both the transmitter and receiver have CSI, they select those antennas that allow a maximization of the capacity. That is,

$$C_{sel} = \max_i \log_2 \left[\det \left(I_L + \frac{\rho}{P} \mathbf{H}_i \mathbf{H}_i^H \right) \right], \tag{2.23}$$

where $\mathbf{H}_i$s are created by deleting $M - P$ columns and $N - L$ rows from $\mathbf{H}$. The optimal algorithms involve an exhaustive search over all possible combinations

$S(\tilde{\mathbf{H}})$. Due to the difficulty of providing CSI to the transmitter, antenna selection is done in the receiver side. It is shown in [20] that the upper bounds on the capacity of a system with receive antenna selection approach the full-complexity system's capacity if the number of selected antennas is equal to or greater than M. The search space grows exponentially with N even if antennas selection is employed in the receiver side. Consequently, Gorokhov [21] proposed a suboptimal selection algorithm that a significantly decreases of the computational complexity.

2.5.2 Minimizing Error rate approach

Assuming OSTBC transmission over the antennas, Gore et al. [19] have shown that the SER depends on the received SNR. Since the received SNR relates to the normal Frobenious norm of the selected sub-channel matrix, the optimal antenna sub-set would be

$$\tilde{\mathbf{H}}_{opt} = \arg\max_{i} \|\mathbf{H}_i\|_F^2. \tag{2.24}$$

Note that in this case, exact CSI or statistical channel knowledge is available at the transmitter or receiver. In [22] and [23], the authors extended this work to any type of space time codes and presented an approximate analysis of the PEP for antenna selection. These authors showed that by selecting an antenna sub-set based on (2.24), the diversity order is maintained whereas the coding gain is reduced.

In some specific cases where the channel rapidly varies, estimation of the channel is either too costly or almost impossible. Therefore, a technique that does not require the CSI either at the receiver or at the transmitter is needed for selecting antennas. Without CSI, the authors of [24] proposed an interesting technique for antenna selection at the receiver. Based on this technique, a subset of receive antennas with the largest received signal powers are chosen. For single antenna selection, the rule is given by

$$n_{opt} = \arg\max_{n=1,\cdots,N} z_n, \tag{2.25}$$

where $z_n = \mathbf{y}_n^H \mathbf{y}_n$ is the norm of the received signal at the nth receive antenna ($\mathbf{y}_n$). The authors of [24] further applied this rule to USTM and proved the full diversity order can be achieved by this selection criterion. In Chapter 5, this scheme is comprehensively reviewed, and several extensions are provided.

2.6 Decoding Techniques

Along with designing ST codes and analyzing MIMO system capacity, decoding techniques for ST codes have received much attention. As mentioned in (2.5), when the channel matrix $\mathbf{H}$ is known to the receiver, $\widehat{S}$ is the ML solution if it minimizes $\Lambda(\mathbf{S}) = \|\mathbf{Y} - \mathbf{HS}\|_F^2$ (Y is the received matrix) over all possible transmitted codewords. Since no explicit analytic solution exists for this problem, an exhaustive search is required on all possible transmitted matrices. Nevertheless, because of its computational complexity, an exhaustive search is computationally prohibitive in most cases.

Fast decoding is another possible way to find transmitted codeword by relaxing the entries of $\mathbf{S}$ and first using the inverse (or pseudo inverse) of the channel matrix $\mathbf{H}$ to calculate $\widetilde{\mathbf{S}} = \mathbf{H}^{-1}\mathbf{Y}$ and then mapping each entry of $\widetilde{\mathbf{S}}$ to the nearest point in the signal constellation [25], [26]. This method leads to a sub-optimum decoding technique called the Zero-Forcing (ZF) decoder or Decorrelator. Although the ZF decoder is much less complex than the ML decoder and can be implemented easily, it suffers from weak performance. The ZF decoder can be modified to find the inverse channel matrix by using more reliable and stable numerical methods and also to improve the system performance [27], [28]. For OSTBCs [29], ML decoding can be decoupled into an individual search on each element of $\mathbf{S}$.

Another popular decoding strategy proposed along with V-BLAST is known as nulling and canceling, which gives a reasonable tradeoff between complexity and performance. The matrix inversion process in nulling and canceling is performed in layers: one estimates a row from S, subtracts the symbol estimates from Y, and keeps on decoding successively [25]. Full details and analysis of this approach are provided in [30].

Instead of exhaustive search on all possible transmitted matrices, ML decoding can be implemented by efficiently searching the solution space. This method is called sphere decoding and has recently been discussed extensively in the literature [31] and [32]. Sphere decoding is based on the enumeration of the lattice points located within a hypersphere of some radius centered at a target, e.g., the received

signal point. This methods' complexity depends on the method used for determining the subset of the signal matrices in particular and the SNR of the system in general.

2.7 Summary

This chapter defined some important concepts of a MIMO system such as space time codes, diversity order, coding gain and spatial rate. Three different channel models that are frequently assumed in the literature were presented along with an introduction to USTM and DUSTM. Antenna-selection techniques and selection rules for different transmission schemes were briefly reviewed. Finally, some well-known decoding techniques including ML and Non-ML techniques for ST codes were discussed.

Chapter 3

Differential Unitary Space-Time Code design

This chapter begins with a brief introduction to unitary ST code design. Two new constellations of unitary matrices and an approximation of union bound on the symbol error probability (SEP) as a design criterion are introduced in Section 3.2. By using an exhaustive search, the optimum codes with integer parameters are found and in Section 3.4 their performance is examined in terms of the SER. By using the Genetic Algorithm technique, a powerful global optimization method, the optimum codes with real parameters are found. The simulation results for these codes' error rate performance are presented in Section 3.5.

3.1 Introduction

As mentioned before, DUSTM has been proposed for use with an unknown, slow, flat-fading MIMO channel [7], [17]. The signal constellation consists of a set of unitary matrices, and the design objective is to maximize the diversity product among all the members of the unitary constellation. Achieving this design goal leads to the minimization of the block error probability in the high signal-to-noise ratio (SNR) region.

Based on maximizing the diversity product, several unitary constellations have been proposed [2], [33], [34]. The design in [2] results in cyclic diagonal matrices with M parameters, where M is the number of transmit antennas. The parameters are numerically optimized to maximize the diversity product. In [33] and [34], the

cyclic design is augmented with additional multiplying matrices and the design of [33] is limited to three to six transmit antennas. Instead of maximizing the diversity product, Wang et al. [35] minimized the union bound on the block error probability by taking into consideration the number of receive and transmit antennas and the operating SNR.

In Section 3.2, two new unitary signal constellations are derived: a simple generalization of [33] and a constellation based on [36]. When M is even, the first is a special case of the second. An approximate union bound on PEP is derived. Optimal codes with integer parameters are searched and found to minimize the union bound. For larger MIMO dimensions or higher data rate, finding the optimum code by exhaustive search over all possible integer design-parameters might be almost impossible. In Section 3.5, the relaxation of the design parameters to the real numbers is investigated and the genetic algorithm method is used to solve the resulting optimization problem. The simulation results show that by relaxing the design parameters, better codes for DUSTM are found.

3.2 Code Design Criteria and Approximate Union Bound

In Section 2.2.1 and 2.4, the system model and the DUSTM scheme are described. To transmit a data sequence of integers $d_1, d_2, \ldots$ with $d_t \in \{0, \ldots, L-1\}$, each d_t is mapped to a distinct unitary matrix signal $\mathbf{\Phi}_{d_t}$ drawn from a unitary space-time matrix constellation $\mathcal{V}$; i.e., $\mathcal{V} = \{\mathbf{\Phi}_1, \mathbf{\Phi}_2, \cdots, \mathbf{\Phi}_L\}$. The data rate is given by $R = \log_2 L/M$.

Assuming that the channel remains constant for at least two block intervals (i.e., $\mathbf{H}_t = \mathbf{H}_{t-1}$), the pairwise error probability (PEP) is given by [35]

$$P_{ll'} = p(\mathbf{\Phi}_l \to \mathbf{\Phi}_{l'}) = \frac{1}{\pi} \int_0^{\frac{\pi}{2}} \prod_{i=1}^{M} \left(1 + \frac{\gamma \lambda_i}{4 \sin^2 \theta}\right)^{-N} d\theta, \tag{3.1}$$

where $\gamma = \frac{\rho^2}{1+2\rho}$, and $\{\lambda_i\}$ is the i-th eigenvalue of the matrix $\mathbf{\Delta}_{ll'} = (\mathbf{\Phi}_l - \mathbf{\Phi}_{l'})(\mathbf{\Phi}_l - \mathbf{\Phi}_{l'})^H$.

For asymptotically high SNR, [7] and [37] show that the design criterion is to

maximize the *diversity product* ζ to minimize PEP; i.e.,

$$\zeta(\mathcal{V}) = \frac{1}{2} \min_{l \neq l'} |\det(\mathbf{\Phi}_l - \mathbf{\Phi}_{l'})|^{\frac{1}{M}}. \tag{3.2}$$

On the other hand, for low SNR, the design criterion is to maximize the trace product, which is called *diversity sum* [35] which is defined as

$$\xi = \min_{l \neq l'} ||\mathbf{\Phi}_l - \mathbf{\Phi}_{l'}||^2. \tag{3.3}$$

In [35], instead of the diversity product, the union bound on the block error probability is the design objective. To help achieve this objective, an easy-to-compute approximation of the PEP is derived for the rapid evaluation of the union bound.

By substituting $\sin\theta = t$ in (3.1) and using the Gaussian quadrature rules [38], the PEP (3.1) may be expressed as

$$P_{ll'} = \frac{1}{2n} \sum_{i=1}^{n} \frac{1}{\det[I + \frac{\gamma}{4x_i^2}\Delta_{ll'}]^N} + R_n \tag{3.4}$$

where $x_i = \cos(2i-1)\pi/2n$ and R_n is a reminder term. Our numerical experiments showed that the choice of about 9 terms ($n = 9$) is sufficient for the remainder term to be negligible. Since the above PEP is very accurate, it can be combined with the union bound on the overall block error probability. For all equally-likely $\mathbf{\Phi}_l$, the union bound becomes

$$P_{UB} \simeq \frac{1}{18L} \sum_{l=0}^{L-1} \sum_{l \neq l'}^{L-1} \sum_{i=1}^{9} \frac{1}{\det[I + \frac{\gamma}{4x_i^2}\Delta_{ll'}]^N}. \tag{3.5}$$

Unlike the diversity product, which ignores the SNR, (3.5) takes into account the operational SNR and the number of receive antennas. Thus, minimizing the union bound (3.5) may be a useful design objective.

3.3 Unitary Constellation Design

The two new signal constellations are developed next, and several of their properties are described. Consider the rotation matrix given by

$$RF_M(\underline{k}\theta) = \begin{pmatrix} RF_2(k_1\theta) & \dots & 0 \\ \vdots & \ddots & \\ 0 & \dots & RF_2(k_{\frac{M}{2}}\theta) \end{pmatrix}_{M \times M}, \tag{3.6}$$

where

$$RF_2(k_i\theta) = \begin{pmatrix} \cos k_i\theta & \sin k_i\theta \\ -\sin k_i\theta & \cos k_i\theta \end{pmatrix},$$

and $\underline{k} = \{k_1, k_2, \ldots, k_{\frac{M}{2}}\}$ is a set of different rotation factors. Our proposed DUSTM constellation $\mathcal{V} = \{\Phi_l | l = 0, \ldots, L-1\}$ consists of the following unitary matrices:

$$\Phi_l = \begin{pmatrix} e^{j\theta_L\mu_1} & \ldots & 0 \\ \vdots & \ddots & \vdots \\ 0 & \ldots & e^{j\theta_L\mu_M} \end{pmatrix}^l .[RF_M(\underline{k}\theta_L)]^l, \tag{3.7}$$

where $l = 0, \ldots, L-1$, and $\theta_L = \frac{2\pi}{L}$. Clearly, a $M \times M$ unitary matrix can be parameterized by $\frac{3M}{2}$ parameters. When all k_is are the same, our proposed constellation reduces to the *cyclic rotated design*, which was proposed in [34]. When all k_is are set to zero, (3.7) reduces to the *cyclic diagonal design* in [2]. Since our constellation has more parameters, a better performance than that of the previous designs is expected. For example, our constellation outperforms those in [34] and [2] in terms of the maximum diversity product. In comparison to [33], our constellation is simple and is available for any even number of transmit antennas M (not limited to $M \leq 6$). However, like the constellation in [34], it is restricted to the MIMO systems with an even number of transmit antennas.

In our proposed designs, we need to find the optimum set of parameters $\underline{\mu} = \{\mu_1, \cdots, \mu_M\}$ and $\underline{k} = \{k_1, \cdots, k_{\frac{M}{2}}\}$ that yield the largest diversity product (3.2) or the smallest union bound (3.5), depending on the case. Since analytical determination of the optimums appears intractable, either an exhaustive computer search or genetic algorithms are used to find the optimum parameters. We first introduce a general unitary matrix constellation based on [36] that can successfully handle both an even or odd number of transmit antennas, and also include (3.7) as a special case. Note that the unitary signals in (3.7) and the proposed constellation in [34] are limited to an even number of transmit antennas. This constellation has M phase angles $\mu_1, \cdots, \mu_M$ and $M-1$ rotation angles $k_1, \cdots, k_{M-1}$ and is given by

$$\begin{aligned} \Phi_l = & \begin{pmatrix} e^{j\theta_L\mu_1} & \ldots & 0 \\ \vdots & \ddots & \vdots \\ 0 & \ldots & e^{j\theta_L\mu_M} \end{pmatrix}^l .[\mathbf{J}_{1,2}(k_1\theta_L)]^l \\ & .[\mathbf{J}_{2,3}(k_2\theta_L)]^l \cdots [\mathbf{J}_{M-1,M}(k_{M-1}\theta_L)]^l \end{aligned} \tag{3.8}$$

, where

$$\mathbf{J}_{i,i+1}(k_i\theta_L) = \begin{pmatrix} \mathbf{I}_{i-1} & 0 & \cdots & 0 \\ 0 & \cos(k_i\theta_L) & -\sin(k_i\theta_L) & 0 \\ \vdots & \sin(k_i\theta_L) & \cos(k_i\theta_L) & \vdots \\ 0 & \cdots & 0 & \mathbf{I}_{M-i-1} \end{pmatrix}, \tag{3.9}$$

$\theta_L = \frac{2\pi}{L}$, and $l = 0, \ldots, L-1$. When all k_i are set to zero, (3.8) is exactly the same as the diagonal cyclic constellation of [2], and in the case of even transmit antenna, if all k_{2j}, $j = 1, \ldots, \frac{M-2}{2}$, are set to zero, (3.9) is an extension of the constellation (3.7).

3.4 Exhaustive Computer Search

Here, an exhaustive computer search is employed to find the optimum parameters. To reduce the computational complexity, all design parameters are restricted to integer numbers. Thus, candidates for the best set of $\underline{\mu}$ and $\underline{k}$ are exhaustively generated and examined for performance (maximum ζ or minimum P_{UB}) and hold if they act better than the previous best candidate set. Since the computational complexity grows exponentially with M and L, one can reduce the search complexity by applying the following theorems.

Theorem 3.4.1 *For an even number of transmit antennas, the diversity product between the lth and l'th unitary matrices in (3.7) depends only on* $(l' - l) \mod L$.

Proof 3.4.1 *By substituting constellation (3.7) in formula (3.2), the diversity product can be written as*

$$\begin{aligned} \zeta_{ll'} &= \frac{1}{2}|\det(\mathbf{\Phi}_l - \mathbf{\Phi}_{l'})|^{\frac{1}{M}} \\ &= \frac{1}{2}\prod_i |1 - (e^{j\Delta_l\Theta_L\mu_i} + e^{j\Delta_l\Theta_L\mu_{i+1}})\cos(k_i\Delta_l\Theta_L), \\ &\qquad + e^{j\Delta_l\Theta_L(\mu_i+\mu_{i+1})}|^{\frac{1}{M}} \end{aligned} \tag{3.10}$$

where $1 \leq i \leq M-1$, *i is odd, and* $\Delta_l = l' - l$. *It is clear, therefore, that* $\zeta_{ll'}$ *depends only on the difference between l and l'. As a result, it is sufficient to consider* $\zeta_{0l'}$ *for* $l' = 1, 2, \cdots, L-1$ *to find the diversity product for a particular sets of parameter* $\underline{\mu}$ *and* $\underline{k}$.

Theorem 3.4.2 *Assume all the conditions of theorem 3.4.1, $\underline{\mu}$ and $\underline{k}$ should be in either of the following forms:*

1. *All μ_i's are even numbers, while all k_i's are odd numbers.*

2. *All μ_i's are odd integers number, and all k_i's are even integer numbers.*

Proof 3.4.2 *See [34]. The same argument is applied here by taking into account the different rotation angles instead of just one rotation angle.*

Note that the above theorems cannot be extended to the constellation (3.8). However, by invoking the following theorem, the search complexity can be reduced.

Theorem 3.4.3 *For a proposed unitary matrix $\mathbf{\Phi}_l$ in (3.8), if L is an even number, at least one parameter must be an odd number among all parameters $\underline{\mu} = \{\mu_1, \cdots, \mu_M\}$ and $\underline{k} = \{k_1, \cdots, k_{M-1}\}$.*

Proof 3.4.3 *Suppose that all parameters $\underline{k}$ and $\underline{\mu}$ are even integer numbers. Thus, we observe that $\mathbf{\Phi}_0$ and $\mathbf{\Phi}_{\frac{L}{2}}$ are viewed as the same at the receiver and,consequently, the receiver will not be able to identify whether $\mathbf{\Phi}_0$ or $\mathbf{\Phi}_{\frac{L}{2}}$ was transmitted. Consequently, this set of parameters does not result in the minimum upper bound on PEP or the maximum diversity product.*

In order to further reduce the search space, one can decrease the number of independent parameters in the constellation (3.8). Of course, the achievable diversity product may decrease as well. Following an idea from [34], if M is even,

$$\tilde{\mu}_k = \begin{cases} \mu_1 + 2(k-1) & 1 \leq k \leq \frac{M}{2}, \\ \mu_2 + 2k - M - 2 & \frac{M}{2} < k \leq M \end{cases} \tag{3.11}$$

and when M is odd,

$$\tilde{\mu}_k = \begin{cases} \mu_1 + 2(k-1) & 1 \leq k \leq \frac{M-1}{2}, \\ \mu_2 & k = \frac{M+1}{2}, \\ \mu_3 + 2k - M - 1 & \frac{M+1}{2} < k \leq M. \end{cases} \tag{3.12}$$

The maximum diversity products of our proposed codes in (3.8), the codes in [34], and the cyclic diagonal codes in [2] are presented in Table 3.1 for a system

M	L	$\zeta(proposed)$	ζ(in [34])	cyclic
6	16	0.5946	0.5946	0.5066
	32	.5577	.5069	0.448
10	16	0.5946	0.5946	0.5623
	32	.5655	.5137	0.5131

Table 3.1: Diversity Product of the optimum codes with different constellation scheme $M = 6$, $N = 1$, $L = 16, 32$

Scheme/criterion	$\underline{\mu}$	$\underline{k}$	P_{UB}
Diag./ min P_{UB}	$[1, 3, 7]$	$[-, -]$	$5.746e{-4}$
Rot./ max ζ	$[10, 10, 9]$	$[3, 12]$	$2.310e{-4}$
Rot./ min P_{UB}	$[7, 7, 10]$	$[12, 4]$	$1.799e{-4}$

Table 3.2: Comparison of constellation parameters and Union bound for rotated and diagonal signal , $M = 3, N = 2, L = 16$

with 6 or 10 transmit and single receive antennas. and a constellation size of 16 and 32. As we expected, our proposed constellation has an equal or higher diversity product relative to the other constellations.

Table 3.2 presents the optimum codes found the from search based on optimizing the diversity product and minimizing the upper bound for our proposed constellation (3.8) and the diagonal cyclic scheme in [2]. The system parameters are $M = 3$ transmit antennas and $N = 2$ receive antennas and the operating SNR= 12. Note that reference [34] does not provide any code for 3 transmit antenna systems. Due to continuity, the optimum code in a particular SNR is either optimum or near optimum code within a range of SNR. To show the coding advantage of our design, we list the P_{UB} of the all the optimum codes. We observe that the union bound of our proposed constellation is less than that of the original designs.

3.4.1 Simulation Results and Discussion

Codes in Table 3.2 and optimum codes for constellation size $L = 8$ are simulated. The proposed constellation in (3.7) with different rotation angles (2 rotation angles for $M = 3$) performs better than the previously proposed constellations. Fig 3.1 shows that by applying new constellation and union-bound criteria, a coding gain

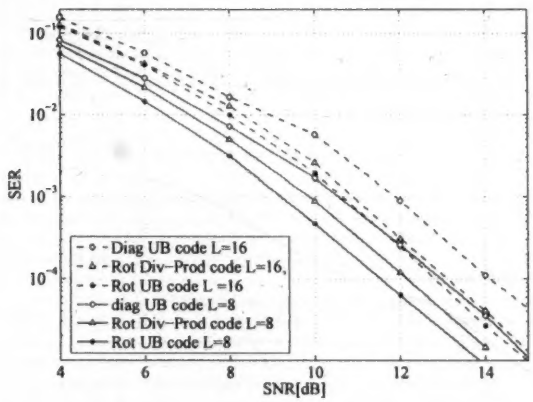

Figure 3.1: Symbol Error Rate of two different constellation with $M = 3$, $N = 2$ for Differential receiver.

about 1.5 dB is achieved over the code designed in [2] at an SER of 10^{-4}. A slow fading channel with Jakes' fading model is assumed in which normalized fading parameters $f_d T_s = 1.5 \times 10^{-3}$. f_d is the Doppler frequency and T_s is the sampling period. The union-bound based design generally has better performance than the design based on the diversity product in both constellations.

3.5 Genetic Algorithm Search method

The design parameters $\underline{\mu}$ and $\underline{k}$ are obtained based on the criteria mentioned in Section 3.2. Without loss of generality, we assume that a set of parameters should be optimized by minimization of a cost function. Previously, when the design parameters were restricted to integers, an exhaustive computer search or random search for optimum parameters was employed since analytical determination of the optimum appeared to be intractable. Moreover, because the computational complexity increases exponentially with M and L, using an exhaustive search to find the optimum parameters for large L and M is difficult. A random search, does not guarantee that the final outputs are close to an acceptable neighborhood of the optimum parameters.

To handle these problems, we employ a genetic algorithm to extract the optimal parameters. Although it does not guarantee the global optimality of its answers,

the cost of genetic solutions are better than the optimum values from an exhaustive search. This seemingly contradictory result is obtained by relaxing the design parameters to be real in the genetic search rather than to be integer parameters assumed in the exhaustive search. This extension embeds the integer parameter space in a much larger real parameter space, improving the likelihood of finding better codes. In the following sections, the genetic algorithm is described and the experimental results are provided.

3.5.1 Genetic Algorithms

The genetic algorithm [39] is an exceptional search technique for finding approximate solutions to optimization and search problems based on natural selection, the process that drives biological evolution. To use a genetic algorithm, a method of representing a solution (encoding the solution) is required such that it can be manipulated by the algorithm. Usually, solutions are represented as binary strings of 0s and 1s, but different encodings are also possible. Additionally, we require the fitness function (cost function) to measure the quality of any solution.

The algorithm begins by creating a random initial population and then making a sequence of new populations/generations. In each generation, the fitness of the whole population is evaluated, and a score is assigned to each member of the current population. Each member with higher associated fitness value is given a higher score. A selection mechanism based on the given scores is applied to the population and the individuals strive for survival. The fitter individuals have more chance to be selected to produce the next generation by means of genetic transformations such as crossover and mutation. Because the entire population participates in the search, the genetic algorithm is less likely than many search procedures to get stuck at a local minimum. As the algorithm continues, and newer and newer generations evolve, the quality of solutions improves.

In general, the next generation is composed of three types of children as follows:

Elite Children: Children in the current generation are selected for the next generation based on their fitness values. Since the selection rule here is probabilistic, not deterministic, fitter solutions (measured by a fitness function) are typically more

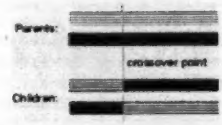

Figure 3.2: one-point crossover technique

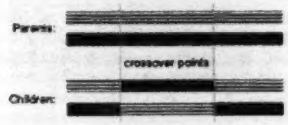

Figure 3.3: two-points crossover technique

likely to be selected. The non-determined rule helps to keep the diversity of the population large and also avoids convergence to a poor solution as well.

M	L	ζ (genetic)	ζ(exhaustive)	cyclic
6	16	0.6602	0.6083	0.5066
	32	0.5678	0.5069	0.448
8	16	0.6601	0.6153	0.5623
	32	0.5827	0.5453	0.5221

Table 3.3: Diversity products of DUST codes obtained by genetic algorithm and exhaustive search.

Crossover Children: These are created by combining pairs of parents in the current population. Typically, the new solution shares many characteristics of the 'parents.' Generally, the crossover operation recombines the selected solutions (parents), by swapping part of them, producing divergent solutions to explore the search space. Many crossover techniques exist to produce a child of a pair of parents [40]. However, all of them are surprisingly simple to implement, involving random number generation and partial string exchanges. Figures 3.2 and 3.3 illustrate the two different techniques used in crossover generation.

The scattered crossover function is another technique usually used in crossover generation. This method first creates a random binary vector with the same size of parents. Then if the ith bit is 0, the corresponding gene is selected from the first parent; otherwise, this gene is selected from the second parent. Ultimately, all the selected genes are combined to form the child. For example, if p_1 and p_2 are the

Table 3.4: Implementation parameters for GA

Population size(p)	700	Stall generation limit	200
Time Limit	5 hours	Crossover fraction	0.8
Mutation type	Uniform	Crossover type	Scattered
N_g	1e5	Parameters bound	LB=0, UB=2π

parents, $p_1 = [a, b, c, d, e, f, g, h]$, $p_2 = [1, 2, 3, 4, 5, 6, 7, 8]$, and the binary vector is $[1, 1, 0, 0, 1, 0, 0, 0]$, the function returns the following child:

$$child = [a, b, 3, 4, e, 6, 7, 8].$$

Mutation Children: The algorithm generates mutation children by randomly changing the bits (genes) of an individual parent in the current generation. This process can be carried out by adding a random vector from a Gaussian distribution to the parent. The aim of mutation is to allow the algorithm to avoid local optima by preventing the population from becoming too similar to each other, thus slowing or even stopping evolution.

As a result, new mutated members along with new crossover members and the rest of those selected from the previous population form the new generation. The genetic algorithm uses the following conditions to terminate:

- A solution is found that satisfies the criteria(Fitness limit).
- Allocated time is reached (Time limit).
- The specified number of generations is reached.
- No improvement occurs in the objective function for a specific number of successive iterations.

The GA implementation parameters, which were used in our program, have been presented in Table 3.4. For more details, refer to [41]. Table 3.3 shows the parameter search results and their corresponding diversity product for the signal constellation in [34] for $L = 16$ and 32, and $M = 6$ and 8, obtained from the genetic algorithm. For comparison, the diversity product of the obtained codes in [34] and [2],

obtained from the exhaustive integer search, are included in Table 3.3. With the use of parameter relaxation and genetic search, almost all results are better than those from the exhaustive search. Clearly, to find the optimum parameters in our proposed constellations in (3.7) and (3.8), the genetic algorithm can be used as well.

Remark: In some cases, the extracted parameters from the exhaustive search seem to be the global optimum answer. However, to our knowledge, the literature provides no proof for this conclusion.

3.5.2 Simulation Results and Discussion

For comparison, the performance results for DUSTM codes from genetic algorithms and the exhaustive integer search are given.

Fig. 3.4 displays the SEP for the proposed constellations in [2] and [34] with the integer parameters obtained from the exhaustive search along with the real parameters obtained from the genetic search. In our simulations, the Rayleigh fading channel was used with Jakes' model with a normalized fade rate of $f_d T_s = 2.5 \times 10^{-3}$. The performance was for a MIMO system with $M = 6$ and $N = 1$ for $L = 16$ and 32. Fig. 3.4 clearly shows that the codes extracted by the genetic search outperformed the previous results obtained by an exhaustive search. The performance improvement is about 0.4 dB for the cyclic group design and 0.6 dB for the cyclic-rotated design, at a 10^{-5} error rate.

3.6 Summary

This chapter introduced the two new constellations of unitary matrices for DUSTM and searched for the optimum parameters based on minimizing the union bound on the SEP. A closed-form approximation of the union bound which is much easier to compute was derived. Although the number of independent parameters involved in our proposed constellation (3.8) is more than those of cyclic rotated and diagonal constellations, its error performance is considerably better. In addition, our proposed unitary constellation, unlike cyclic rotation, can be employed in any MIMO system with an arbitrary number of transmit antennas. In Section 3.5, by using

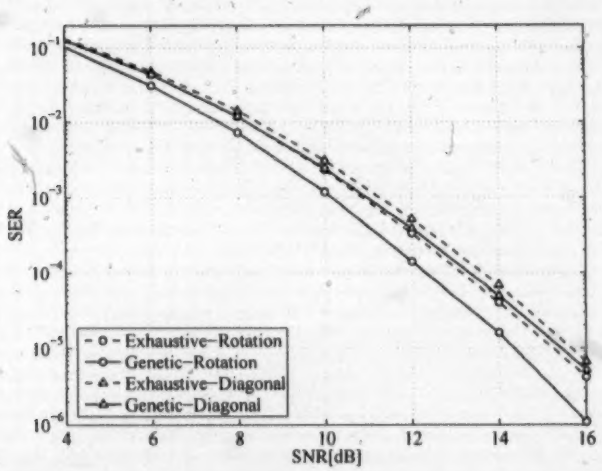

Figure 3.4: Symbol Error Rate performance of cyclic and cyclic rotated design when $L = 16$, $M = 6$ and $N = 1$. The dashed line curves are for exhaustive search and solid lines are for genetic search.

the Genetic algorithm and relaxing the parameters to the real numbers rather than integers, the performance of the cyclic rotated and diagonal codes in terms of maximizing the diversity product or minimizing the union bound was improved.

Chapter 4

Optimum Design DUSTM for Transmit-Correlated Channel

In this chapter, a DUSTM design criterion for the transmit-correlated Rayleigh fading channel is presented. Using the unitary matrix constellations introduced in Section 3.3, in Section 4.3 we search for the constellation parameters to minimize the union bound on SEP by taking into account the number of receive and transmit antennas, the operational SNR, and the correlation matrix. Section 4.4 examines the performance of the ML (optimal) receiver and differential (suboptimal) receiver and quantifies the influence of the correlation coefficient on the coding gain.

4.1 Introduction

As mentioned before DUSTM is suitable for use where neither the transmitter nor the receiver knows the wireless channel [6]. The design criteria and performance analysis in terms of symbol error rate (SER) for DUSTM scheme over the independent-fading channels have been extensively investigated in the literature [2], [34], [35]. However, a few works address the performance analysis of unitary space time modulation (USTM) scheme in general and the DUSTM scheme in particular, operating over spatially correlated channels. The error performance of USTM has been derived for correlated channels [42]. In this present work, we assume that a correlation exists between any pairs of only transmit antennas. This assumption is realistic since in many practical multiantenna system with sufficient antenna spacing, the channel gain associated with different transmit antennas ex-

hibit strong correlations whereas correlation between receive antennas is negligible [12]. Reference [43] shows that the channel correlation matrix is independent of the operation environment and is just a function of the mobile angular position with respect to the transmitter. As a result, the knowledge of the correlation matrix can be estimated at the receiver even though the channel coefficients vary rapidly.

In this chapter, a design criterion to construct the differential codebook of unitary matrices is presented for the spatially-correlated channel case. Using the unitary-matrix constellations introduced in the previous chapter, we search for the optimum constellation parameters that minimize the union bound on SEP by taking into account the number of receive and transmit antenna, the operational SNR, and the correlation matrix. In the simulation section, the performance of the ML (optimal) decoder and differential (suboptimal) decoder is investigated. The simulation results show that the suboptimal decoders's performance approaches the optimal's performance at the high region of SNRs. Because of the availability of the correlation knowledge at the receiver, both optimal and suboptimal decoders can be implemented. However, due to the lower complexity of the differential (suboptimal) decoder, this decoder is more desirable for use than the optimal decoder, especially at medium or high SNRs.

4.2 DUSTM over Transmit Correlation

Consider a MIMO system introduced in Section 2.2.1 with M transmit and N receive antennas signaling over a correlated flat-fading channel. As described in Section 2.4, DUSTM is a special case of unitary modulation obtained by rewriting $\mathbf{Y} = [\mathbf{Y}_{t-1}^T \mathbf{Y}_t^T]$, $\tilde{\mathbf{\Phi}}_{z_t} = 1/\sqrt{2}[\mathbf{I}_M, \mathbf{\Phi}_{z_t}^T]^T$ and $\mathbf{W} = [\mathbf{W}_{t-1}^T \mathbf{W}_t^T]^T$. Hence, the input-output relationship in this case reduces to

$$\mathbf{Y} = \sqrt{2\rho}\tilde{\mathbf{\Phi}}\mathbf{H} + \mathbf{W}. \tag{4.1}$$

Note that $T = 2M$ is chosen to derive the equation (4.1). To model the correlation between antennas, the spatially transmit-correlation model is employed, $\mathbf{H} = \mathbf{R}_T^{1/2}\mathbf{H}_w$ where $\mathbf{H}_w$ is an $M \times N$ matrix composed of i.i.d. $\mathcal{CN}(0,1)$ RVs, and the matrix $\mathbf{R}_T$ specifies transmit correlation matrix (2.3.1). The ML decoder in

this case would be

$$\tilde{z}_t = \arg \max_{0 \le l < L} \operatorname{tr} \left\{ \mathbf{Y}^H \tilde{\mathbf{\Phi}}_l (\frac{1}{2\rho} \mathbf{R}_T^{-1} + \mathbf{I}_M)^{-1} \tilde{\mathbf{\Phi}}_l^H \mathbf{Y} \right\}. \tag{4.2}$$

On the other hand, by using the fundamental differential receiver equation given in [2], the differential estimator regardless of the channel type would be

$$\tilde{z}_t = \arg \min_{0 \le l < L} \|\mathbf{Y}_t - \mathbf{\Phi}_l \mathbf{Y}_{t-1}\|_F^2. \tag{4.3}$$

Neither estimator (4.2) nor estimator (4.3) requires the CSI. However, the former estimator, which needs the correlation matrix $\mathbf{R}_T$ to extract the data, is actually a ML decoder while the latter decoder is not. We will investigate the performance of these two estimators in terms of the SEP and the system complexity.

4.2.1 Pairwise Error Probability in case of DUST Code

The exact pairwise error probability of USTM under the correlated fading channel assumption has been derived in [42]. Generally, the PEP is a function of the operational SNR, N, M and the channel correlation matrix $\mathbf{R}_T$ in a very complicated manner. By using $\mathbf{R}_H = \mathbf{I}_N \otimes \mathbf{R}_T$, the PEP of DUSTM may be expressed as

$$P\{\mathbf{\Phi}_l \to \mathbf{\Phi}_{l'}\} = -\sum_{\mathrm{Re}(r_k)<0} \mathrm{Res}_{s=1/r_k} \left\{ \frac{1}{s \prod_{k=1}^{2M} (1 - r_k s)^N} \right\}, \tag{4.4}$$

where $r_1, \ldots, r_{2M}$ are the eigenvalues of

$$\begin{aligned} \mathbf{C}_{l,l'} &= \left(\mathbf{I}_{2M} + 2\rho \tilde{\mathbf{\Phi}}_{l'} \mathbf{R}_T \tilde{\mathbf{\Phi}}_{l'}^H \right)^{-1} (\tilde{\mathbf{\Phi}}_l \mathbf{R}_T \tilde{\mathbf{\Phi}}_l^H - \tilde{\mathbf{\Phi}}_{l'} \mathbf{R}_T \tilde{\mathbf{\Phi}}_{l'}^H) \\ &= 2\rho \left[-\mathbf{I}_{2M} + (\mathbf{I}_{2M} + 2\rho \tilde{\mathbf{\Phi}}_{l'} \mathbf{R}_T \tilde{\mathbf{\Phi}}_{l'}^H)^{-1} (\mathbf{I}_{2M} + 2\rho \tilde{\mathbf{\Phi}}_l \mathbf{R}_T \tilde{\mathbf{\Phi}}_l^H) \right]. \end{aligned} \tag{4.5}$$

In (4.5), $\tilde{\mathbf{\Phi}}_l = \frac{1}{\sqrt{2}} [\mathbf{I}_M, \mathbf{\Phi}_l^T]^T$ and $\tilde{\mathbf{\Phi}}_{l'} = \frac{1}{\sqrt{2}} [\mathbf{I}_M, \mathbf{\Phi}_{l'}^T]^T$. Note that the probability of mistaking $\mathbf{\Phi}_l$ for $\mathbf{\Phi}_{l'}$ is not necessarily equal to the probability of mistaking $\mathbf{\Phi}_l'$ for $\mathbf{\Phi}_l$ in a correlated channel.

4.3 Code Design

Reference [44] argues the optimum DUST codes for the Rayleigh channel case must yield the minimization of the union bound on PEP. Similarly, the same approach can

be drawn and applied to the correlated channel case. Hence, if Φ_ls are equally likely to be transmitted, a good criterion for a code design is to minimize the union bound

$$P_{UB} = \frac{1}{L}\sum_{l=0}^{L-1}\sum_{l'\neq l} P\{\Phi_l \rightarrow \Phi_{l'}\}, \tag{4.6}$$

which is obtained by summing the Chernoff bounds of all the PEPs divided by L.

In order to construct the unitary codebook, along with a design measure, an unitary constellation is required. An elegant constellation of unitary matrices for the DUSTM systems was proposed in Section 3.3. These codes not only yield better performance than other codes in terms of lower SEP but also can be applied to a MIMO system with an arbitrary number of transmit antennas. For the given codebook size $L \geq 2$, M, N and the operational SNR, an exhaustive search is performed to obtain the best set of integer parameters $\underline{\mu} = \mu_1, \cdots, \mu_M \in \{0, \ldots, L-1\}$ and $\underline{k} = k_1, \ldots, k_{M-1} \in \{0, \ldots, L-1\}$ that minimizes the P_{UB}. Since to the best of our knowledge, no explicit solution exists for this problem, an exhaustive computer search is employed. Candidates for the best set of $\underline{\mu}$ and $\underline{k}$ are exhaustively generated and tested in a performance measure (4.6) and kept if they are better than the previously best candidate set. Below, it is shown that by using the following theorems, the search-space complexity of our proposed constellation as well as some other constellations can be significantly reduced. We then compare the error performance of the optimum codes obtained from our proposed scheme with the codes resulting from other available constellations in the literature.

Theorem 4.3.1 *Considering the diagonal constellation in [2], the eigenvalues of matrix* $\mathbf{C}_{l,l'}$ *are the same as the eigenvalues of* $\mathbf{C}_{0,k}$ *where* $k = (l' - l) \mod L$. *As a result, it is sufficient to compute* $\mathbf{C}_{0,l}$ *and* $\mathbf{C}_{l,0}$ *for* $l = 1, 2, \cdots, L-1$ *to calculate the union bound in (4.6).*

Proof 4.3.1 *Let's define* $\mathrm{eig}(\mathbf{C}_{l,l'})$ *as the set of eigenvalues of the matrix* $\mathbf{C}_{l,l'}$. *From (4.5), we have*

$$\mathrm{eig}(\mathbf{C}_{l,l'}) = \frac{1}{2\rho}\left([-1, \cdots, -1]^T + \mathrm{eig}\left[(\mathbf{I}_{2M} + 2\rho\tilde{\mathbf{\Phi}}_l\mathbf{R}_T\tilde{\mathbf{\Phi}}_l^H)^{-1}(\mathbf{I}_{2M} + 2\rho\tilde{\mathbf{\Phi}}_{l'}\mathbf{R}_T\tilde{\mathbf{\Phi}}_{l'}^H)\right]\right). \tag{4.7}$$

By using the matrix inversion and determinant Lemmas, i.e., $(\mathbf{A}+\mathbf{BCD})^{-1} = \mathbf{A}^{-1} - \mathbf{A}^{-1}\mathbf{B}(\mathbf{C}^{-1}+\mathbf{D}\mathbf{A}^{-1}\mathbf{B})^{-1}\mathbf{D}\mathbf{A}^{-1}$ *and* $\mathrm{eig}(\mathbf{AB}) = \mathrm{eig}(\mathbf{BA})$, *equation (4.7) can be rewritten as*

$$\mathrm{eig}(\mathbf{C}_{l,l'}) = \frac{1}{2\rho}\left([-1,\cdots,-1]^T + \mathrm{eig}\left[(\mathbf{I}_{2M} - 2\rho(\mathbf{\Lambda}^{-1}+2\rho\mathbf{I}_{2M}))^{-1}(\mathbf{I}_{2M} - 2\rho\mathbf{P}\mathbf{\Lambda}\mathbf{P}^H)\right]\right), \tag{4.8}$$

where $\mathbf{P} = \mathbf{U}^H(\mathbf{I}_M + \mathbf{\Phi}_{l'}^H\mathbf{\Phi}_l)$, *and* $\mathbf{U}$ *and* $\mathbf{\Lambda}$ *result from the SVD decomposition of* $\mathbf{R}_T = \mathbf{U}\mathbf{\Lambda}\mathbf{U}^H$. *Due to the orthogonal structure of* $\mathbf{\Phi}_l$ *and* $\mathbf{\Phi}_{l'}$, *we have* $\mathbf{P} = \mathbf{U}^H(\mathbf{I}_M + \mathbf{\Phi}_k^H\mathbf{\Phi}_0)$, *where* $k = (l'-l) \mod L$. *Therefore,* $\mathrm{eig}(\mathbf{C}_{l,l'}) = \mathrm{eig}(\mathbf{C}_{0,k})$.

Theorem 4.3.2 *For the general unitary matrix* $\mathbf{\Phi}_l$ *in (3.8), if* L *is an even number, among all parameters* $\underline{\mu} = \{\mu_1,\cdots,\mu_M\}$ *and* $\underline{K} = \{k_1,\cdots,k_{M-1}\}$, *at least one parameter must be an odd number.*

Proof 4.3.2 *Proof by contradiction; Consider* $\mathbf{C}_{0,\frac{L}{2}}$, *when* $k_i = \text{even}$ *for* $i = 1,\cdots,M$ *and* $\mu_j = \text{even}$ *for* $j = 1,\cdots,M-1$, *then* $\mathbf{C}_{0,\frac{L}{2}} = \mathbf{0}_{2M\times 2M}$. *In this case,* $\mathbf{\Phi}_0$ *and* $\mathbf{\Phi}_{\frac{L}{2}}$ *are viewed as the same at the receiver, and, consequently, the receiver will not be able to identify whether* $\mathbf{\Phi}_0$ *or* $\mathbf{\Phi}_{\frac{L}{2}}$ *was transmitted. This set of parameters definitely does not result in the minimum upper bound on SEP.*

In constellation (3.8), $2M-1$ parameters should be determined. The computational complexity and, accordingly, the time needed for finding the optimum parameters grows exponentially with the increase of M and L. Following an idea from [34], we further reduce the search space by decreasing the number of independent parameters in the diagonal matrix of (3.8), if M is even:

$$\tilde{\mu}_k = \begin{cases} \mu_1 + 2(k-1) & 1 \le k \le \frac{M}{2}, \\ \mu_2 + 2k - M - 2 & \frac{M}{2} < k \le M, \end{cases} \tag{4.9}$$

and when M is odd,

$$\tilde{\mu}_k = \begin{cases} \mu_1 + 2(k-1) & 1 \le k \le \frac{M-1}{2}, \\ \mu_2 & k = \frac{M+1}{2}, \\ \mu_3 + 2k - M - 1 & \frac{M+1}{2} < k \le M. \end{cases} \tag{4.10}$$

In the next section, the performances of some optimized DUST codes based on different constellations for a spatial correlated channel are presented. We also

L	Our code	P_{UB}	Cyclic group code	P_{UB}
8	$\underline{\mu} = [2,2,2], \underline{k} = [4,5]$	0.02027	$\underline{\mu} = [2,7,3]$	0.02247
16	$\underline{\mu} = [7,7,10], \underline{k} = [4,5]$	0.0607	$\underline{\mu} = [1,12,9]$	0.0625

Table 4.1: Optimum codes and their corresponding union upper bound based on proposed constellation in (3.8) and diagonal (cyclic) constellation in [2], $M = 3, N = 1, SNR = 14dB$

investigate how the correlation coefficient between each two antennas affects the coding gain. The correlation model considered in this section is the exponential correlation model introduced in Section 2.3.1.

For illustration purposes, we present an example of a MIMO system with $M = 3\ N = 1\ \gamma = .9$ and then construct the different unitary codebooks associated with each unitary constellations. Note that, $\mathbf{R}_T$ should be normalized so that $E\{|h_{i,j}|^2\} = 1$. Table 4.1 shows the obtained parameters of the proposed unitary constellation in (2.3.1) along with the optimum parameters of the diagonal unitary constellation for codebook size $L = 8, 16$. Their corresponding union bounds for each group of codes are also presented for comparison purpose.

Note that the optimum codes which lead to the minimum upper bound might change for different SNRs. However, due to continuity, we expect that a code with minimum P_{UB} in a particular SNR is still the optimum code or very close to the optimum code within a range of SNR.

4.4 Simulation Results

By using the obtained codes in Table 4.1, the symbol error rate (SER) performance of the ML receiver (4.2) and Non-ML (Differential) receiver is shown in Fig. 4.1 as a function of the received SNR. Moreover, this figure depicts the performance of the proposed codes in (2.3.1), the diagonal codes that optimized the union bound in (4.6) and the diagonal code in [2] designed for the Rayleigh-fading channel when $M = 3$, $N = 1$, $L = 16$. By taking into account the channel correlation model, we observe that the new design of the diagonal constellation achieves a coding advantage of about .4 dB at the SER range $10^{-2} - 10^{-3}$ over the code designed in [2]

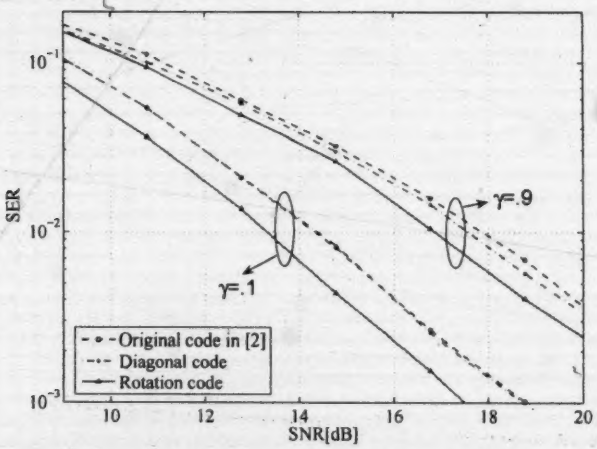

Figure 4.1: Symbol Error Rate of two different constellation with $M = 3$, $N = 1$ for ML receiver and Non-ML(Differential) receiver.

where the correlation was not considered . By using our proposed constellation in (3.3) to construct the codebook, a better performance compared to the others is obtained such that, for instance, this improvement is approximately 1 dB at an SER of 2×10^{-3}. As SNR increases, the performance of the differential (Non-ML) decoder approaches the performance of the ML decoder. This point is more obvious in Fig. 4.2, which depicts the SER performance of the optimum codes with a different correlation matrix assumption for $M = 2$, $N = 2$, $L = 8$ and $\mathbf{R}_T = \begin{bmatrix} 1 & \gamma \\ \gamma & 1 \end{bmatrix}$.

Fig. 4.2 illustrates the SER performance of the optimum codes for different values of the correlation coefficient (γ), assuming $M = 2$, $N = 2$, $L = 8$.

Both ML and Non-ML detectors perform identically when no correlation exist between the transmit antennas ($\gamma = 0$). This result was expected because in [2], it is proved that in the case of the Rayleigh-fading channel (no spatially correlation), differential detection is actually equivalent to ML detection. We notice that even though the correlation coefficient is not zero, e.g., $\gamma = 0.5$, the performances of the ML and differential decoders are very similar. This fact implies that a differential decoder with so much less complexity can be used instead of a ML decoder in a practical system and that a differential decoder exhibits the same error rate performance.

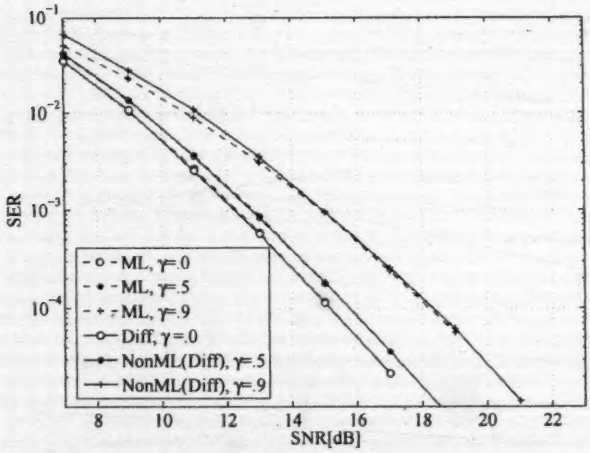

Figure 4.2: Performance comparison of ML and Non-ML receivers on the optimum code in constellation (2.3.1) when $M = 2$, $N = 2$ and $L = 8$.

4.5 Summary

In this chapter, we investigated the error rate performance of the DUSTM scheme operating over a transmit-correlated fading channel. In such a system, to construct the best unitary codebook, we introduced a design measure that minimizes the union bound. As expected, our optimum codes showed a better performance than those of the existing codes for the correlated channel case. In the simulation section, the performance of ML and differential decoders was studied, and it was observed that the differential decoder's performance approaches the ML's performance at high SNR.

Chapter 5

Antenna Selection for USTM over Correlated and Ricean Channels

Section 5.2 describes the system model and presents a brief overview of USTM and DUSTM. In Section 5.3, the ML decoder and Chernoff bound on PEP are derived for antenna selection and USTM over the correlated fading channel. For two transmit correlation models, the diversity order and coding gain are derived. The extension of our performance analysis to the Ricean channel is presented in Section 5.4. The numerical results are shown in Section 5.5, and concluding remarks are given Section 5.6. Lastly, in Appendix A.3, we investigate the convergence behavior of some available CDFs of the quadratic forms and compare them with our derived formula in terms of the Minimum Square Error (MSE).

5.1 Introduction

Most previous USTM studies assumed that all the available antennas are utilized for signal transmission and reception [35], [18], [45]. However, each active transmit/receive antenna pair requires an RF (radio frequency) chain, which is expensive. Consequently, antenna selection, where a subset of all available antennas are selected at the transmitter and/or receiver, has been extensively studied [20], [46], [47]. However, most previous research on antenna selection considers coherent multi-antenna systems in which perfect CSI is available at the receiver [48, 49].

The only study that deals with USTM and receive antenna selection (RAS) without CSI is [24]. Its main contribution is the derivation of the diversity order and

coding gain via the Chernoff bound on the PEP for USTM and RAS. It is shown that a MIMO system employing USTM and RAS achieves full spatial diversity. However, [24] considers only independent Rayleigh fading MIMO channels. In reality, insufficient antenna spacing, angle spread or the lack of rich scattering may cause spatial correlation among antennas, particularly at the transmit side [12], [50]. Moreover, channel measurements reveal that in some propagation environments, a fixed (possibly line of sight (LoS)) component [11] is present. In this case, the mean of the channel matrix is not zero, and the channel is modeled by the Rician fading channel.

In this chapter, the analysis of [24] is extended to independent Ricean and correlated fading channels. RAS is based on the instantaneous received signal power. The optimal decoders for both channel assumptions are presented, and then the associated Chernoff bounds on the PEP are derived based on the optimal decoders when a single antenna is selected. Both the exponential and constant correlation models are considered in our work. Since our performance analysis is for the high-SNR region, the most important contribution in this work is to derive the most dominant term of the CDF's power series of the received signal power at any receiver with respect to SNR. We further show that the convergence behavior of our CDF expression is much better than that of the other CDF expressions available in other studies such as [1] or [51], [52].

Our analytical results indicate that the full diversity is preserved in both correlated and Ricean fading channels for USTM and RAS. However, the correlations result in a loss in the coding gain while a higher K-factor improves the performance.

5.2 System Model and USTM Scheme

Consider a MIMO system with M transmit and N receive antennas signaling over a frequency flat-fading channel. As described in Section (2.2.1), the received matrix signal is written as [6]

$$\mathbf{Y}_\tau = \sqrt{\frac{\rho}{M}}\mathbf{S}_\tau\mathbf{H} + \mathbf{W}_\tau, \tag{5.1}$$

where $\mathbf{Y}_\tau = [\mathbf{y}_1, \ldots, \mathbf{y}_N]$ is a $T \times N$ complex received signal matrix, $\mathbf{S}_\tau$ is a $T \times M$ complex transmitted signal matrix, and $\mathbf{W}_\tau$ denotes a $T \times N$ additive noise matrix with i.i.d. $\mathcal{CN}(0,1)$ elements, and the block-time index is τ. Moreover, the $M \times N$ random channel matrix $\mathbf{H}$ consists of a fixed (line of sight [LOS]) component and a random (diffuse) component. The channel may be represented as

$$\mathbf{H} = \sqrt{\frac{K}{K+1}}\overline{\mathbf{H}} + \sqrt{\frac{1}{K+1}}\mathbf{R}_T^{1/2}\mathbf{H}_w. \tag{5.2}$$

The Ricean factor K indicates the relative strength of the LoS component over the diffuse component, providing an indication of link quality [16].

Two special cases of (5.2) are investigated below. The correlated channel model without a LOS component ($K = 0$ and $\mathbf{R}_T \neq \mathbf{I}_M$) is considered next, and the Ricean channel model without a correlation ($K \neq 0$ and $\mathbf{R}_T = \mathbf{I}_M$) will be treated in Section 5.4.

5.3 Error Probability of USTM RAS in Correlated Fading

In this section, the performance of the USTM RAS in a correlated channel is analyzed. The antenna selection rule and the decoding algorithm are described. The Chernoff bound on the PEP is derived for the case selecting the 'best' single antenna.

The selection rule here is a commonly used way of selecting a receive antenna by using a simple maximum-norm detection circuit. This rule does not require the receiver to know the the CSI or even the correlation matrix. The rule is that an antenna whose received signal norm is the largest among all the antennas is selected [24]; i.e,

$$\hat{n} = \arg \max_{n=1,2,\ldots,N} z_n, \tag{5.3}$$

where $z_n = \|\mathbf{y}_n\|^2$.

For this selection rule, the Chernoff bound on the PEP of mistaking $\mathbf{\Phi}_l$ for $\mathbf{\Phi}_{l'}$ is expressed as [24]

$$P_{\text{CB}}(\mu) = \frac{1}{2}\int_{\mathcal{C}^T} \frac{NF_z(\mathbf{y}^H\mathbf{y})^{N-1}}{\det(\pi\mathbf{R}_l)^{1-\mu}\det(\pi\mathbf{R}_{l'})^{\mu}} \times \exp\Big\{-\mathbf{y}^H\{\underbrace{\mu\mathbf{R}_{l'}^{-1} + (1-\mu)\mathbf{R}_l^{-1}}_{\mathbf{\Omega}(\mu)}\}\mathbf{y}\Big\}d\mathbf{y},$$

where $0 \leq \mu \leq 1$ is a free parameter that is chosen to minimize $P_{\text{CB}}(\mu)$. $F_z(.)$ denotes the cumulative density function (CDF) of $\|\mathbf{y}\|^2$, and $\mathbf{R}_l$ and $\mathbf{R}_{l'}$ are the $T \times T$ covariance matrices conditioned on $\mathbf{\Phi}_l$ and $\mathbf{\Phi}_{l'}$ transmitted, respectively. The covariance matrix $\mathbf{R}_l$ can be written as

$$\mathbf{R}_l = \mathrm{E}(\mathbf{y}_i \mathbf{y}_i^H) = \mathbf{I}_T + \frac{\rho T}{M} \mathbf{\Phi}_l \mathbf{R}_T \mathbf{\Phi}_l^H. \tag{5.4}$$

Note that each antenna at the receiver observes independently correlated-fading gains from the transmitter antennas provided that no correlation between the receive antennas exists. As a result, all the columns of the received signal $\mathbf{Y}$ are i.i.d.. By using the matrix inversion and determinant lemmas in [6], one can derive

$$\mathbf{R}_l^{-1} = \mathbf{I}_T - \mathbf{\Phi}_l \big(\mathbf{I}_M + (\frac{\rho T}{M} \mathbf{R}_T)^{-1}\big)^{-1} \mathbf{\Phi}_l^H \tag{5.5}$$

and

$$\det(\mathbf{R}_l) = \det(\mathbf{I}_M + \frac{\rho T}{M} \mathbf{D}), \tag{5.6}$$

where the diagonal matrix $\mathbf{D} = \mathrm{diag}\{\lambda_1, \ldots, \lambda_M\}$ is obtained from the singular value decomposition of $\mathbf{R}_T$.

Let us define $p_{\mathbf{y}_{\hat{n}}}(\mathbf{y}_{\hat{n}} | \mathbf{\Phi}_l)$ as the probability density function (PDF) of the signal in selected antenna $\hat{n}$. By considering the selection rule , the ML detection rule is given by

$$\mathbf{\Phi}_{\text{ML}} = \arg \max_{\mathbf{\Phi}_l \in \{\mathbf{\Phi}_1, \ldots, \mathbf{\Phi}_L\}} p_{\mathbf{y}_{\hat{n}}}(\mathbf{y}_{\hat{n}} | \mathbf{\Phi}_l). \tag{5.7}$$

Using the theory of order statics in [53] and considering the fact that $F_z(\|\mathbf{y}\|^2)$ is independent of the transmitted signal $\mathbf{\Phi}_l$ (this independence will be proven shortly), the decision rule (5.7) can be simplified as

$$\mathbf{\Phi}_{\text{ML}} = \arg \max_{\mathbf{\Phi}_l \in \{\mathbf{\Phi}_1, \ldots, \mathbf{\Phi}_L\}} \left\{ \hat{\mathbf{y}}^H \mathbf{\Phi}_l \left(\mathbf{I}_M + (\frac{\rho T}{M} \mathbf{D})^{-1} \right)^{-1} \mathbf{\Phi}_l^H \hat{\mathbf{y}} \right\}. \tag{5.8}$$

If we assume that the receiver knows the correlation matrix, ML detection requires searching over the codebook $\mathcal{V}$ in order to choose the optimum signal by maximizing (5.8). Note that although the RAS criterion in (5.7) does not require the correlation matrix $\mathbf{R}_T$, the optimal detection rule in (5.8) requires $\mathbf{R}_T$ in order to extract the most likely transmitted signal.

To compute P_{CB} in (5.4), $F_z(\|\mathbf{y}\|^2)$ is required. This CDF can be obtained by the Laplace-transform inversion of the moment generating function (MGF) of $\|\mathbf{y}\|^2$ given by [54, page 595]:

$$G(s) = \frac{1}{\det(\mathbf{I}_T + s\mathbf{RF})}, \tag{5.9}$$

where $\mathbf{F} = \mathbf{I}_T$ and $\mathbf{R} = \mathbf{I}_T + \frac{\rho T}{M}\mathbf{\Phi}\mathbf{R}_T\mathbf{\Phi}^H$ is the receive covariance matrix. The transmit correlation matrix can take several forms. Two popular correlation models for $\mathbf{R}_T$ are considered in Section 2.3.1. Extensive use is made of the eigenvalues of the correlation matrices in (2.11) and (2.12) in the following.

5.3.1 Exponential Correlation Case

For the exponential correlation model, the CDF of $z_n = \|\mathbf{y}_n\|^2$, denoted by $F_z(a)$ throughout the paper, is derived here. The CDF is used to derive the performance of USTM and RAS in terms of the diversity order and coding gain. We will use some of the results in [24], [6], and the rotational property of the Vandermonde matrix [55].

First, we will briefly outline the derivation procedure. The diversity order and coding gain are meaningful only in the asymptotically high SNR region. Typically, to find these, the Chernoff bound on the error probability is derived as a power series of the SNR. The diversity order and coding gain are then extracted from this power series. For example, at asymptotically high SNRs, if the following relation [56],

$$P_{\text{CB}} = (G_c\rho)^{-G_d} + o(\rho^{-G_d}), \tag{5.10}$$

holds for the error probability or the Chernoff bound, then G_d and G_c represent the diversity order and coding gain, respectively. In order to evaluate P_{CB} at high SNR ($\rho \to \infty$), the dominant term in the power series expansion of $F_z(a)$ in terms of ρ is required.

With the use of partial fractions, one can expand (5.9) to

$$G(s) = \frac{1}{(1+s)^{T-M}\prod_{i=1}^{M}\left[1+s(\underbrace{\frac{\rho T}{M}\lambda_i+1}_{r_i})\right]}$$

$$= \sum_{k=1}^{T-M}\frac{A_k}{(1+s)^k} + \sum_{k=1}^{M}\frac{B_k}{\left[1+s(\underbrace{\frac{\rho T}{M}\lambda_k+1}_{r_k})\right]}, \tag{5.11}$$

where

$$A_{T-M-k} = \frac{1}{k!}\frac{\partial^k}{\partial s^k}\left(\prod_{i=1}^{M}[1+sr_i]^{-1}\right)\Big|_{s=-1} \tag{5.12a}$$

$$B_k = \left(\frac{1}{1-\frac{1}{r_k}}\right)^{T-M}\prod_{i=1,i\neq k}^{M}\left(1-\frac{r_i}{r_k}\right)^{-1}. \tag{5.12b}$$

The PDF of z_n can be obtained by taking the inverse Laplace transform of (5.11) as follows:

$$f_z(u) = \mathcal{L}^{-1}\{G(s)\}$$

$$= \sum_{k=1}^{T-M}A_k\frac{1}{(k-1)!}u^{k-1}e^{-u} + \sum_{k=1}^{M}\frac{B_k}{r_k}e^{-u/r_k}. \tag{5.13}$$

By integrating (5.13), the CDF of z_n is obtained as

$$F_z(a) = \sum_{k=1}^{T-M}A_k\left(1-e^{-a}\sum_{i=0}^{K-1}\frac{a^i}{i!}\right) + \sum_{k=1}^{M}B_k\left(1-e^{-a/r_k}\right). \tag{5.14}$$

Notice that the CDF expression of $F_z(a)$ in (5.14) is independent of the transmitted signal Φ_l. By inserting (5.12b) into (5.14) and after some manipulations, the second term of the right side of (5.14) approaches to

$$\sum_{k=1}^{M}B_k\left(1-e^{-a/r_k}\right) \to -\sum_{j=1}^{\infty}\frac{(-aM)^j}{(\rho T)^j j!}\times\sum_{k=1}^{M}\lambda_k^{-j}\prod_{i=1,i\neq k}^{M}\left(1-\frac{\lambda_i}{\lambda_k}\right)^{-1}. \qquad \rho\to\infty. \tag{5.15}$$

when $\rho \to \infty$. Upon cursory examination of (5.15), one might conclude that the dominant term occurs at $j = 1$ as $\rho \to \infty$. However, the most dominant term in the power series of $F_z(a)$ is the term ρ^{-M} because the coefficient of any power term ρ^j, $j < M$, is zero.

Theorem 5.3.1 *For any M distinct eigenvalues $\lambda_1, \ldots, \lambda_M$ and $0 < j < M$, the following holds:*

$$\sum_{k=1}^{M} (\lambda_k)^{-j+M-1} \prod_{i=1, i\neq k}^{M} (\lambda_k - \lambda_i)^{-1} = 0. \tag{5.16}$$

Proof 5.3.1 *With the common denominator $\prod_{1\leq i<j\leq M}(\lambda_i - \lambda_j)$, the numerator of the left side of (5.16) would be*

$$\sum_{k=1}^{M} (-1)^{k-1} \lambda_k^{-j+M-1} \prod_{\substack{1\leq i<j\leq M \\ i,j\neq k}} (\lambda_i - \lambda_j) =$$

$$\det \begin{bmatrix} \lambda_1^{-j+M-1} & \lambda_2^{-j+M-1} & \cdots & \lambda_M^{-j+M-1} \\ 1 & 1 & \cdots & 1 \\ \lambda_1 & \lambda_2 & \cdots & \lambda_M \\ \lambda_1^2 & \lambda_2^2 & \cdots & \lambda_M^2 \\ \vdots & \vdots & \cdots & \vdots \\ \lambda_1^{M-2} & \lambda_2^{M-2} & \cdots & \lambda_M^{M-2} \end{bmatrix}. \tag{5.17}$$

The right side of (5.17) arises from the use of the rotational properties of the Vandermonde Matrix (see Section 6.1 [55]) and the general definition of the determinant as well. The left side of (5.17) is now equal to **zero** *for all integers $1 \leq j \leq M-1$ because if j is in this interval, the introduced matrix (5.17) has two equal rows, so its determinant clearly must be zero.*

Thus, the second term of (5.14) is expanded as

$$\sum_{k=1}^{M} B_k \left(1 - e^{-a/r_k}\right) = -\frac{(-aM)^M}{\rho^M T^M M!} \sum_{k=1}^{M} \lambda_k^{-M} \times \prod_{\substack{i=1 \\ i\neq k}}^{M} \left(1 - \frac{\lambda_i}{\lambda_k}\right)^{-1} + o(\rho^{-M}). \tag{5.18}$$

Similarly, the dominant term of the first term of (5.14) is ρ^{-M} as $\rho \to \infty$.

Theorem 5.3.2 *For any integer k, and for large ρ, the following holds:*

$$\frac{\partial^k}{\partial s^k} \left(\prod_{i=1}^{M} [1 + s r_i]^{-1} \right) \Bigg|_{s=-1} = C_k \rho^{-M} + o(\rho^{-M}), \tag{5.19}$$

where C_k is a constant value, independent of ρ, and uniquely determined for each k. In other words, the left side of (5.19) behaves as $C_k \rho^{-M}$ when ρ is sufficiently large.

Proof 5.3.2 *See Appendix A.2.*

In the high-SNR regime, $F_z(a)^{N-1}$ can be approximated by retaining the first term in the power series expansion of $F_z(a)$; thus,

$$F_z(a)^{N-1} = \frac{1}{\rho^{M(N-1)}}\left[\sum_{k=1}^{T-M}\mathcal{D}_k(1-e^{-a}\sum_{i=0}^{K-1}\frac{a^i}{i!}) + a^M\mathcal{E}\right]^{N-1} + o(\rho^{-M(N-1)}), \tag{5.20}$$

where

$$\mathcal{D}_k = C_{T-M-k}\frac{(-1)^{T-M-k}}{(T-M-k)!}$$

$$\mathcal{E} = \left(\sum_{k=1}^{M}(-1)^{M+1}\frac{M^M}{T^M M!\lambda_k^M}\prod_{\substack{i=1\\ i\neq k}}^{M}\left(1-\frac{\lambda_i}{\lambda_k}\right)^{-1}\right). \tag{5.21}$$

Therefore, by substituting (5.6) and (5.20) in (5.4), we obtain

$$P_{\text{CB}}(\mu) = \frac{1}{2}\frac{N}{\pi^T\prod_{i=1}^{M}\left(1+\frac{\rho T}{M}\lambda_i\right)}\int_{\mathcal{C}^T}\left[e^{-\mathbf{y}^H\mathbf{\Omega}(\mu)\mathbf{y}}\times\frac{1}{\rho^{M(N-1)}}\left(\sum_{k=1}^{T-M}\right.\right.$$

$$\left.\left.\mathcal{D}_k(1-e^{-\mathbf{y}^H\mathbf{y}}\sum_{i=0}^{K-1}\frac{(\mathbf{y}^H\mathbf{y})^i}{i!}) + (\mathbf{y}^H\mathbf{y})^M\mathcal{E}\right)^{N-1}\right]d\mathbf{y} + o(\rho^{-MN}). \tag{5.22}$$

From (5.5), $\mathbf{\Omega}(\mu)$ may be rewritten as

$$\mathbf{\Omega}(\mu) = \mathbf{I}_T - \mu\mathbf{\Phi}_{l'}(\mathbf{I}_M + (\frac{\rho T}{M}\mathbf{R}_T)^{-1})^{-1}\mathbf{\Phi}_{l'}^H - (1-\mu)\mathbf{\Phi}_l(\mathbf{I}_M + (\frac{\rho T}{M}\mathbf{R}_T)^{-1})^{-1}\mathbf{\Phi}_l^H,$$

which reduces to

$$\lim_{\rho\to\infty}\mathbf{\Omega}(\mu) = \mathbf{I}_T - \mu\mathbf{\Phi}_{l'}\mathbf{\Phi}_{l'}^H - (1-\mu)\mathbf{\Phi}_l\mathbf{\Phi}_l^H. \tag{5.23}$$

For all $\mathbf{\Phi}_l$ and $\mathbf{\Phi}_{l'}$ drawn from the unitary constellation $\mathcal{V}$, $\text{rank}(\mathbf{\Omega}(\mu)) = T$ for all $l \neq l'$ (i.e. the full diversity constellation). By using the singular value decomposition $\mathbf{\Omega}(\mu) = \mathbf{Q}\,\text{diag}\{\alpha_1,\ldots,\alpha_T\}\mathbf{Q}^H$ in (5.23) and changing the variables $x_t = |\overline{y}_t|^2$, where $\overline{y}_t$ is the t-th element of vector $\mathbf{Q}^H\mathbf{y}$, the Chernoff bound on PEP (5.22) is obtained. Therefore, the diversity and coding gain of USTM and RAS are

$$G_d = MN \tag{5.24}$$

$$G_c = \left(\frac{NM^M}{2T^M\det(R_T)}\int_0^\infty\cdots\int_0^\infty\left[e^{-\sum_{t=1}^{T}\alpha_t x_t}\left(\sum_{k=1}^{T-M}\mathcal{D}_k\left(1-e^{-\sum_{t=1}^{T}x_t}\sum_{i=0}^{k-1}\frac{\left(\sum_{t=1}^{T}x_t\right)^i}{i!}\right)\right.\right.$$

$$\left.\left.+\left(\sum_{t=1}^{T}x_t\right)^M\mathcal{E}\right)^{N-1}\right]dx_1\cdots dx_T\Bigg)^{-1/(MN)}. \tag{5.25}$$

As the final result of P_{CB} implies, for high SNR and full rank space-time codes, the diversity order remains the same as that of the full complexity system. However, some loss in the coding gain occurs, depending on the determinant of $\mathbf{R}_T$.

5.3.2 Constant Correlation Case

The analysis here is similar to that in the rest of the the exponential correlation case. $G(s)$ and $F(\cdot)$ will be calculated as follows:

$$G(s) = \sum_{k=1}^{T-M} \frac{A_k}{(1+s)^k} + \frac{B}{1 + s\underbrace{\left\{\rho T/M[(M-1)\gamma + 1] + 1\right\}}_{r_1}} + \sum_{k=1}^{M-1} \frac{C_k}{\left[1 + s\underbrace{(\rho T/M(1-\gamma)+1)}_{r_2}\right]^k}, \tag{5.26}$$

where

$$A_{T-M-k} = \frac{1}{k!}\frac{\partial^k}{\partial s^k}\left(\frac{1}{(1+sr_1)(1+sr_2)^{M-1}}\right)\Big|_{s=-1} = r_1^k \frac{(1-r_2)^{-M}}{(r_1-1)^k} \times \sum_{i=0}^{k} \binom{M+i-2}{i} \left(\frac{r_2}{r_1}\right)^i \left(\frac{1-r_1}{1-r_2}\right)^{i-1} \tag{5.27a}$$

$$B = \left(1 - \frac{1}{r_1}\right)^{-1} \left(1 - \frac{r_2}{r_1}\right)^{1-M} \tag{5.27b}$$

$$C_k = \left(\frac{-r_1}{r_2}\right)^{M-1-k} \left(1 - \frac{r_1}{r_2}\right)^{k-M} \left(1 - \frac{1}{r_2}\right)^{M-T} \times \sum_{i=0}^{M-1-k} \binom{T-M+i-1}{T-M-1} \left[\left(1 - \frac{r_1}{r_2}\right)^{-1} \left(1 - \frac{1}{r_2}\right) r_1\right]^{-i} \tag{5.27c}$$

By taking the inverse Laplace transform of (5.26) and then integrating it with respect to u over $[0, a]$, the final CDF will be given by

$$F_z(a) = \sum_{k=1}^{T-M} A_k \left\{1 - e^{-a} \sum_{i=0}^{k-1} \frac{a^i}{i!}\right\} + B\left(1 - e^{-a/r_1}\right) + \sum_{k=1}^{M-1} C_k \left\{1 - e^{-a/r_2} \sum_{i=0}^{k-1} \frac{(a/r_2)^i}{i!}\right\}. \tag{5.28}$$

Notice that as we expected before both (5.14) and (5.28) are independent of the transmitted signal Φ_l. This condition was necessary to derive the ML decoder introduced in (5.8). As we claimed in exponential correlation case, we first claim here that the dominant term in the power series expansion of $F_z(a)$ shown in (5.28) occurs at the ρ^{-M} term.

Theorem 5.3.3 *For a characteristic function $F_z(a)$ in (5.28), the asymptotic/dominant term in the power series expansion occurs at order of ρ^{-M}; i.e., the first $M-1$ terms of the asymptotic series for $F_z(a)$ are zero.*

Proof 5.3.3 *The argument in the previous correlation matrix case is applied herein as well. The alternative proof for this theorem can be drawn from Eq.(24) of Reference [1].*

What remains is to determine the coefficient of ρ^{-M} in the asymptotic series of $F_z(a)$ in order to present the best approximation of it. As ρ asymptotically goes to infinity and if we substitute (5.27a) in (5.28), the first term in the right side of equation (5.28) reduces to

$$\sum_{k=1}^{T-M} A_k \left\{ 1 - e^{-a} \sum_{i=0}^{k-1} \frac{a^i}{i!} \right\} = \rho^{-M} \frac{(1-\gamma)^{-M+1}(-M)^M}{T^M[(M-1)\gamma+1]} \times \sum_{k=1}^{T-M} \sum_{i=0}^{T-M-k} \binom{M+i-2}{i} \left\{ 1 - e^{-a} \sum_{i=0}^{k-1} \frac{a^i}{i!} \right\} + o(\rho^{-M}), \tag{5.29}$$

which indicates that the power series of the left side of formula (5.29) starts with the ρ^{-M} term. This statement does not apply to the other expressions left in equation (5.28). The second and third terms of $F_z(a)$ might apear to contain $M-1$ first terms in the power series as well such as ρ^{-i}, $i = 1, 2, \ldots, M-1$. In fact, from Theorem 5.3.3, we know in advance that the significant term in $F_z(a)$ is ρ^{-M}; therefore, all ρ^{-i}, $i = 1, 2, \ldots, M-1$ disappear in the power series.

By using the two following identities (5.30) and (5.31),

$$\sum_{j=0}^{M} \frac{(-x)^j}{j!} \sum_{i=0}^{k-1} \frac{x^i}{i!} = 1 - \sum_{j=0}^{M-k} \left(\sum_{i=0}^{j} \frac{(-1)^{j+i}}{(k+i)!(j-i)!} \right) x^{k+j} + o(x^{M+1}), \tag{5.30}$$

$$\sum_{i=0}^{\infty} \binom{\alpha+i}{i} x^i = \frac{1}{(1-x)^{\alpha+1}} \qquad 0 < x < 1, \tag{5.31}$$

in (5.27c) and (5.28), respectively, it can be shown that C_k goes to

$$\lim_{\rho \to \infty} C_k = \left(\frac{-r_1}{r_2}\right)^{M-1-k} \left(1 - \frac{r_1}{r_2}\right)^{k-M} \times \left[1 - \binom{T-k-1}{T-M-1} \left(1 - \frac{r_1}{r_2}\right)^{M-k} \left(\frac{1}{r_1}\right)^{M-k}\right]. \tag{5.32}$$

If we insert C_k of (5.32) into (5.28) and consider only the term ρ^{-M}, and given that this term is the dominant term, the asymptotic $F_z(a)$ in the constant correlation case is given by (5.33), which appears at the bottom of this page.

In order to verify (5.33), Fig. 5.1 shows the empirically obtained CDF of $\|\mathbf{y}^2\|$ along with the first term in the power series expansion of z_n's CDF presented in (5.33). Clearly, we are looking for $F_z(a)$ as a function of ρ and a in order to calculate P_{CB}. As Fig. 5.1 depicts, the difference between the approximation and empirical value exponentially approaches zero as SNR gets sufficiently large. The rest of the procedure to obtain the diversity order and coding gain is the same procedure we carried out in exponential correlated case; By setting $F_z(a)$ from (5.33) in (5.22) accordingly, G_c and G_d can be achieved. In general, the error performance depends on the SNR, the signal constellation and the correlation matrix in a complicated manner. However, it is noted USTM and RAS achieve full spatial diversity (i.e., $G_d = MN$) even with the existence of transmit correlations.

$$F_z(a) = \frac{T^{-M}}{\rho^M} \left[\frac{(1-\gamma)^{-M+1}(-M)^M}{[(M-1)\gamma+1]} \times \sum_{k=1}^{T-M} \sum_{i=0}^{T-M-k} \binom{M+i-2}{i} \left\{1 - e^{-a} \sum_{i=0}^{k-1} \frac{a^i}{i!}\right\} + \right.$$
$$\frac{aM(-a/\gamma)^{M-1}}{M![1+(M-1)\gamma]} - \frac{1-\gamma}{(M-1)\gamma+1} \times \sum_{k=1}^{M-1} \left(\frac{(M-1)\gamma+1}{M\gamma}\right)^{M-k} \left(\frac{M}{1-\gamma}\right)^{M} \times$$
$$\left. \left\{ \sum_{i=0}^{M-1} \frac{a^M(-1)^{i+M-k}}{(K+i)!(M-k-i)!} - \binom{T-k-1}{T-M-1} \left(\frac{-M\gamma}{(M-1)\gamma+1}\right)^{M-k} a^k \right\} \right] + o(\rho^{-M}) \tag{5.33}$$

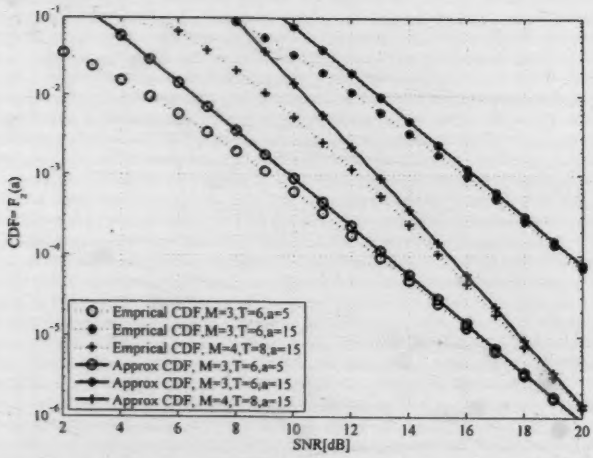

Figure 5.1: Comparison of the approximation and exact curve of $F_z(a)$ assuming constant correlation matrix with $\gamma = 0.5$

5.4 Extension to Ricean-Fading Channels

The performance analysis of USTM and RAS is now extended to Ricean fading channels. Here, spatial correlation is ignored and, the elements of $\mathbf{H}_w$ are assumed to be i.i.d. circularly symmetric complex Gaussian random variables, i.e., $\mathcal{CN}(0,1)$. If the received signal $\mathbf{Y}$ is formulated again as (5.1), and the LOS component has equal effect on each receive antenna, $\mathbf{Y}$ consists of N i.i.d. columns with the $T \times T$ covariance matrix $\mathbf{R}_l$ as

$$\mathbf{R}_l = \mathbf{I}_T + \frac{\rho T}{M(K+1)} \mathbf{\Phi}_l \mathbf{\Phi}_l^H. \tag{5.34}$$

Therefore, the likelihood function of the received signal at the nth antenna, i.e., $\mathbf{y_n}$, can be written as

$$p_{\mathbf{y}_n}(\mathbf{y}|\mathbf{\Phi}_l) = \frac{\exp\left\{-(\mathbf{y}-\overline{\mathbf{y}_l})^H \mathbf{R}_l^{-1}(\mathbf{y}-\overline{\mathbf{y}_l})\right\}}{\pi^T \det(\mathbf{R}_l)}, \tag{5.35}$$

where

$$\overline{\mathbf{y}}_l = \sqrt{\frac{\rho T K}{M(K+1)}}\boldsymbol{\Phi}_l \overline{\mathbf{h}}_n$$
$$\mathbf{R}_l^{-1} = \mathbf{I}_T - \frac{x}{x+1}\boldsymbol{\Phi}_l\boldsymbol{\Phi}_l^H. \tag{5.36}$$

where $x = \frac{\rho T}{M(K+1)}$ hereafter. After some manipulations of the exponent term of (5.35), similar to what we did in the correlated channel case, the ML decoding rule becomes

$$\boldsymbol{\Phi}_{\mathrm{ML}} = \arg\max_{l=1,\ldots,L}\left\{\frac{\rho T}{M}\|\mathbf{Y}^H\boldsymbol{\Phi}_l\|_F^2 + 2\sqrt{\frac{\rho T}{M}K(K+1)}\,\mathrm{tr}\left\{\Re(\mathbf{Y}^H\boldsymbol{\Phi}_l\overline{\mathbf{H}})\right\}\right\}. \tag{5.37}$$

By using the same argument used in [24], it is proved that instead of $\mathbf{Y}$ and $\overline{\mathbf{H}}$ which are, respectively, the received block matrix and the channel fixed component. Thus, we can substitute $\mathbf{y}_n$ and $\overline{\mathbf{h}}_n$ accordingly in (5.37) as the received and LOS vector at the selected antenna whose signal norm is the highest.

5.4.1 Chernoff Bound and Performance Analysis

In this section, the Chernoff bound on PEP is derived for the Ricean channel. The Chernoff bound of mistaking $\boldsymbol{\Phi}_l$ for $\boldsymbol{\Phi}_{l'}$ is given by

$$P_{\mathrm{CB}}(\mu) = \frac{1}{2}\int_{C^T}\frac{NF_z(\mathbf{y}^H\mathbf{y})^{N-1}}{\det(\pi\mathbf{R}_l)^{1-\mu}\det(\pi\mathbf{R}_{l'})^{\mu}}\exp[\xi(\mu|\mathbf{y})]d\mathbf{y}, \tag{5.38}$$

where

$$\xi(\mu|\mathbf{y}) = -\mu(\mathbf{y}-\overline{\mathbf{y}}_{l'})^H\mathbf{R}_{l'}^{-1}(\mathbf{y}-\overline{\mathbf{y}}_{l'}) - (1-\mu)(\mathbf{y}-\overline{\mathbf{y}}_l)^H\mathbf{R}_l^{-1}(\mathbf{y}-\overline{\mathbf{y}}_l).$$

By using the distributive property of matrix algebra, $\xi(\mu|\mathbf{y})$ can be rewritten as

$$\xi(\mu|\mathbf{y}) = -\mathbf{y}^H\underbrace{\left[\mu\mathbf{R}_{l'}^{-1} + (1-\mu)\mathbf{R}_l^{-1}\right]}_{\boldsymbol{\Omega}(\mu)}\mathbf{y} + 2\Re\left\{\mathbf{y}^H[\mu\mathbf{R}_{l'}^{-1}\overline{\mathbf{y}}_{l'} + (1-\mu)\mathbf{R}_l^{-1}\overline{\mathbf{y}}_l]\right\} - \underbrace{\left[\mu\overline{\mathbf{y}}_{l'}^H\mathbf{R}_{l'}^{-1}\overline{\mathbf{y}}_{l'} + (1-\mu)\overline{\mathbf{y}}_l^H\mathbf{R}_l^{-1}\overline{\mathbf{y}}_l\right]}_{\Delta(\mu)}. \tag{5.39}$$

By using (5.36) in (5.39), at high SNR region ($x \to \infty$) which is of interest herein, the second term of $\xi(\mu|\mathbf{y})$ becomes

$$\Re\{\mathbf{y}^H[\mu\mathbf{R}_{l'}^{-1}\overline{\mathbf{y}}_{l'} + (1-\mu)\mathbf{R}_l^{-1}\overline{\mathbf{y}}_l]\} = \Re\{\mathbf{y}^H[\frac{\sqrt{xK}}{1+x}(\mu\mathbf{\Phi}_{l'} + (1-\mu)\mathbf{\Phi}_l)\overline{\mathbf{h}}_n]\} \to 0. \tag{5.40}$$

Furthermore, $\mathbf{\Omega}(\mu)$ and $\Delta(\mu)$ are given by

$$\mathbf{\Omega}(\mu) \to \mathbf{I}_T - [\mu\mathbf{\Phi}_{l'}\mathbf{\Phi}_{l'}^H + (1-\mu)\mathbf{\Phi}_l\mathbf{\Phi}_l^H], \tag{5.41a}$$

$$\Delta(\mu) = \alpha \to K\|\overline{\mathbf{h}}_n\|^2. \tag{5.41b}$$

In order to calculate P_{CB} in (5.38), as we did in the correlated channel case, we need to find the CDF of $z = \|\mathbf{y}\|^2$, i.e., $F_z(a)$, knowing that the mean value of $\mathbf{y}$ is not zero any more. The dominant term of CDF respect to ρ will be inserted into (5.38), so that we can obtain coding gain and diversity order.

Different methods can be used to derive the CDF of a non-central quadratic form over circularly symmetric Gaussian vectors. Since we have to integrate such CDF's over $\mathcal{R}^+$, a fast convergent series is needed. In [1] and [51], three infinite series for the CDF of non-central quadratic forms in complex normal variables have been presented. These series are either hard to find a closed form or very poor in convergence. Below, we propose a new method for calculating the first term in the power extension series of such a CDF and then show that it converges much faster than the other series discussed in the literature and is appropriate for our performance analysis. The convergence properties of these series will be discussed in Appendix A.3.

In the sequel we invoke two commonly used functions in our derivation, which are respectively defined as *The incomplete Gamma function*, i.e., the CDF of the $\chi^2(2n)$ distribution defined as

$$\Gamma(n,a) = \int_0^a \frac{u^{n-1}e^{-u}}{(n-1)!}du = 1 - e^{-a}\sum_{j=0}^{n-1}\frac{a^j}{j!}, \tag{5.42}$$

and *the Pochhammer function* for any integer i, defined as

$$(p)_i = \begin{cases} \frac{\Gamma(p+i)}{\Gamma(p)} = p(p+1)\cdots(p+i-1) & i > 0, \\ 1 & i = 0, \\ \frac{\Gamma(p+1)}{\Gamma(p+i+1)} = p(p-1)\cdots(p+i+1) & i < 0. \end{cases} \tag{5.43}$$

Proof 5.4.1 *See our paper in [57].*

We now state the CDF and its associated power series for the squared norm of $\mathbf{y}$.

Theorem 5.4.1 *The PDF and CDF of the quadratic form $z = \|\mathbf{y}_n\|^2$ over a non-central circularly symmetric Gaussian vector $\mathbf{y}_n$ with the covariance matrix of (5.34) are*

$$f_z(a) = (1+x)^{-M} \sum_{k=0}^{\infty} \frac{(-\alpha)^k}{k!} \times \left\{ \sum_{r=1}^{k+M} A_{k,r} \frac{a^{r-1}e^{-\beta a}}{(r-1)!} + \sum_{r=1}^{T-M} B_{k,r} \frac{a^{r-1}e^{-a}}{(r-1)!} \right\} \tag{5.44}$$

and

$$F_z(a) = (1+x)^{-M} \sum_{k=0}^{\infty} \frac{(-\alpha)^k}{k!} \times \left\{ \sum_{r=1}^{k+M} A_{k,r} \frac{\Gamma(r,\beta a)}{\beta^r} + \sum_{r=1}^{T-M} B_{k,r} \Gamma(r,a) \right\}, \tag{5.45}$$

where $\alpha = \frac{x}{1+x} K \|\overline{\mathbf{h}}_n\|^2$, $\beta = \frac{1}{1+x}$, and the coefficients $A_{k,r}$ and $B_{k,r}$ result from

$$A_{k,r} = \psi_{k+M-r,k}(1, T-M, \beta) \quad r = 1, 2, \ldots, k+M, \tag{5.46a}$$

$$B_{k,r} = \psi_{T-M-r,k}(\beta, k+M, 1) \quad r = 1, 2, \ldots, T-M. \tag{5.46b}$$

Proof 5.4.2 *See our proof in [57].*

Theorem 5.4.2 *The most dominant term in the CDF of Theorem 5.4.1 is ρ^{-M}, i.e.*

$$F_z(a) = \rho^{-M} \times \left(\frac{M(K+1)}{T}\right)^M \sum_{k=0}^{\infty} \frac{(-K\|\overline{\mathbf{h}}_n\|^2)^k}{k!} \times \left\{ \sum_{r=1}^{M} A'_{k,r} \frac{y^r}{r!} + \sum_{r=1}^{T-M} B'_{k,r} \Gamma(r,y) \right\} + o(\rho^{-M}). \tag{5.47}$$

where

$$B'_{k,r} = \psi_{T-M-r,k}(0, k+M, 1)$$
$$A'_{k,r} = \frac{(-1)^{M-r}\Gamma(T-r)}{(M-r)! \times \Gamma(T-M)}. \tag{5.48}$$

Proof 5.4.3 *See our proof in [57].*

If (5.39), (5.41a) and (5.41b) are substituted into the P_{CB} expression in (5.38), we arrive at

$$P_{\text{CB}}(\mu) = \frac{e^{-K\|\overline{\mathbf{h}}_n\|^2}}{2\pi^T} \int_{\mathcal{C}^T} \frac{NF_z(\|\mathbf{y}\|^2)^{N-1}}{(1+x)^M} e^{-\mathbf{y}^H \mathbf{\Omega}(\mu)\mathbf{y}} d\mathbf{y}.$$

Therefore, by using the results of Theorem 5.4.2 and the Lebesgue's dominated convergence theorem, the Chernoff bound at the high SNR region is

$$P_{\text{CB}}(\mu) = \rho^{-MN} \frac{N}{2} \Big(\frac{M(K+1)}{T}\Big)^{MN} e^{-K\|\overline{\mathbf{h}}_n\|^2} \int_0^\infty \cdots \int_0^\infty e^{-\sum_{t=1}^T \alpha_t x_t} \Big(\sum_{k=0}^\infty \frac{(-K\|\overline{\mathbf{h}}_n\|^2)^k}{k!} \times$$
$$\Big\{ \sum_{r=1}^M A'_{k,r} \frac{(\sum_{t=1}^T x_t)^r}{r!} + \sum_{r=1}^{T-M} B'_{k,r} \Gamma(r, \sum_{t=1}^T x_t) \Big\} \Big)^{N-1} dx_1 \cdots dx_T + o(\rho^{-MN}), \tag{5.49}$$

where $\alpha_1, \ldots, \alpha_T$ are all eigenvalues of the matrix $\mathbf{\Omega}(\mu)$, assuming $\text{rank}(\mathbf{\Omega}(\mu)) = T$. Note that equation (5.49) is obtained by changing the variable $x_t = |z_t|^2$ where z_t is the tth element of vector $\mathbf{Q}^H\mathbf{y}$, similar to what occurs in the correlated case. The diversity gain and coding gain are

$$G_d = MN,$$
$$G_c = \Bigg(\frac{N}{2} \Big(\frac{M(K+1)}{T}\Big)^{MN} e^{-K\|\overline{\mathbf{h}}_n\|^2} \int_0^\infty \cdots \int_0^\infty e^{-\sum_{t=1}^T \alpha_t x_t} \Big(\sum_{k=0}^\infty \frac{(-K\|\overline{\mathbf{h}}_n\|^2)^k}{k!}$$
$$\times \Big\{ \sum_{r=1}^M A'_{k,r} \frac{(\sum_{t=1}^T x_t)^r}{r!} + \sum_{r=1}^{T-M} B'_{k,r} \Gamma(r, \sum_{t=1}^T x_t) \Big\} \Big)^{N-1} dx_1 \cdots dx_T \Bigg)^{-1/(MN)}, \tag{5.50}$$

respectively.

Since gaining an insight into the obtained coding gain expression (5.25) is interesting, let us consider a simple 2 by 2 differential unitary space-time case ($T = 4$) for the transmit correlation matrix $\mathbf{R}_T = \begin{bmatrix} 1 & \gamma \\ \gamma & 1 \end{bmatrix}$ and the Ricean channel with

$K = 2$ and $\overline{\mathbf{H}} = \begin{bmatrix} 1 & 1 \\ 1 & 1 \end{bmatrix}$. The direct calculation of (5.12a) and (5.12b) yields

$$\begin{aligned} A_1 &= -\frac{r_1}{(1-r_1)^2(1-r_2)} - \frac{r_2}{(1-r_2)^2(1-r_1)} \to \frac{2}{r_1 r_2} \\ A_2 &= \frac{1}{(1-r_1)(1-r_2)} \to \frac{1}{r_1 r_2}, \qquad \rho \to \infty \\ B_1 &= \frac{1}{(1-1/r_1)^2(1-r_2/r_1)} \\ B_2 &= \frac{1}{(1-1/r_2)^2(1-r_1/r_2)}, \end{aligned} \tag{5.51}$$

where $r_1 = 1 + 2(1+\gamma)\rho$, and $r_1 = 1 + 2(1-\gamma)\rho$. By using the final result of Theorem 5.3.1 and replacing (5.51) and (5.15) into (5.14), $F_z(a)$ in our simple case will be

$$F_z(a) = \frac{1}{4\rho^2(1-\gamma^2)} \left\{ 2(1-e^{-a}) + \left[1 - (1+a)e^{-a}\right] + \frac{a^2}{2} + 2a \right\} + o(\rho^{-2}), \tag{5.52}$$

and eventually from (5.25) and after some simplification, P_{CB} is obtained as

$$\begin{aligned} P_{\text{CB}} &= \frac{1}{16\rho^4}(1-\gamma^2)^{-2} \int_0^\infty e^{-\sum_{t=1}^4 \alpha_t x_t} \left[2(1 - e^{-\sum_{t=1}^4 x_t}) \right. \\ &+ 1 - \left(1 + \sum_{t=1}^4 x_t\right) e^{-\sum_{t=1}^4 x_t} + \frac{(\sum_{t=1}^4 x_t)^2}{2} + 2\sum_{t=1}^4 x_t \Big] \\ &\times dx_1 \cdots dx_4 = \frac{1}{16\rho^4}(1-\gamma^2)^{-2} \Big[- \frac{\sum_{t=1}^4 (\alpha_t + 1)^{-1} + 3}{\prod_{t=1}^4 (\alpha_t + 1)} \\ &+ \frac{1}{\prod_{t=1}^4 (\alpha_t)} \left(3 + \sum_{t=1}^4 \frac{1}{\alpha_t^2} + \sum_{1 \le t < p \le 4} \frac{1}{\alpha_t \alpha_p} - \sum_{t=1}^4 \frac{2}{\alpha_t} \right) \Big] + o(\rho^{-4}). \end{aligned} \tag{5.53}$$

As mentioned earlier, α_i's are the eigenvalues of $\mathbf{\Omega}(\mu)$ defined in (5.23). To determine the optimum μ to minimize P_{CB}, one can use a computer search to find μ_{opt} over interval [0,1]. Note that with transmit correlation, the probability of mistaking $\mathbf{\Phi}_{l'}$ for $\mathbf{\Phi}_l$ is not necessarily equal to the reverse probability. If they are equal, μ must be 1/2 in (5.23).

For the 2×2 Ricean channel, the Chernoff bound in (5.49) is reduced to

$$P_{\text{CB}} = \frac{e^{-2K}}{16\rho^4}(K+1)^4 \sum_{k=0}^{\infty} \frac{(-2K)^k}{k!} \{ \sum_{r=1}^{2} A'_{k,r} \sum_{\substack{l_1,\ldots,l_4, \\ \sum_{i=1}^{4} l_i = r}} \prod_{t=1}^{4} \alpha_t^{-(l_t+1)}$$

$$+ \sum_{r=1}^{2} B'_{k,r} [\prod_{t=1}^{4} \alpha_t^{-1} - \sum_{j=0}^{r-1} \sum_{\substack{l_1,\ldots,l_4, \\ \sum_{i=1}^{4} l_i = j}} \prod_{t=1}^{4} (\alpha_t + 1)^{-(l_t+1)}] \} + o(\rho^{-4}). \qquad (5.54)$$

Proof 5.4.4 *See our proof in [57]*

5.5 Simulation Results

In this section, we examine the correctness of our theoretical analysis by using computer simulation and study the influence of the transmit correlation and K-factor on the error performance of USTM and RAS. To exploit the benefits of differential USTM, the optimized parametric codes in [24] are used in our simulations. Although these codes have been designed for the independent fading channels, numerical experiments show that they are either optimum or near to optimum codes for the correlated/Ricean channel as well. For the sake of simplicity, in our simulation examples we consider a system with two transmit and one or two receive antennas. For antenna selection, we select the best receive antenna based on the maximum received norm. The assumed correlation matrix in our simulation is $\mathbf{R}_T = \begin{bmatrix} 1 & \gamma \\ \gamma & 1 \end{bmatrix}$, and the fixed channel component in Ricean model is given by $\overline{\mathbf{H}} = \begin{bmatrix} 1 & 1 \\ 1 & 1 \end{bmatrix}$.

In Fig. 5.2, we compare the Chernoff bound on PEP presented in (5.53) with simulated PEP for a differential USTM system with $M = 2$, $N = 2$ when a single antenna is selected, $J = 1$. Our theoretical bound is almost 1.5dB away from the exact PEP at PEP equal to 10^{-5} for both the $\gamma = 0.3$ and $\gamma = 0.9$ cases, and it gets tighter at higher SNR. From Fig. 5.3, even for a high level of correlation, e.g. $\gamma = 0.9$. Although some loss occurs in the coding gain, both the full-complexity system and a system employing antenna selection exhibit the same diversity order ($G_d = 4$). To illustrate the advantage of RAS over no antenna selection subject to the same power consumption, we plot the performance of a system with a single receive antenna. As expected, its diversity order is equal to 2. Now, we evaluate the

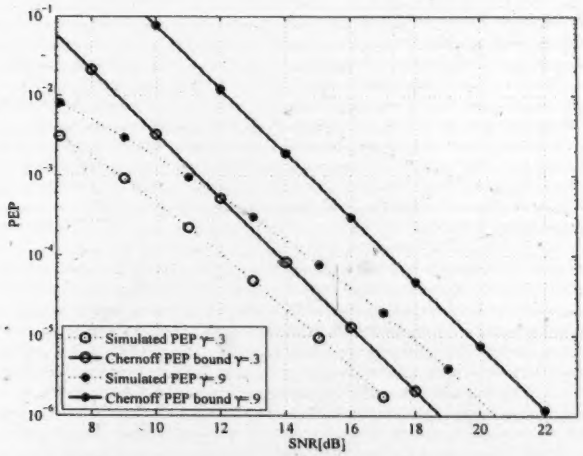

Figure 5.2: Comparison of the Chernoff bound and the simulated PEP with $M = 2$, $N = 2$ $J = 1$

formulation of our performance analysis in the case of a Ricean channel. The exact PEP for $K = 1$, $K = 2$ and $K = 3$ are plotted in Fig. 5.4 along with their associated Chernoff bounds calculated from (5.54). As Fig. 5.4 shows, the higher values of K-factor result in a better system performance. Furthermore, the presented Chernoff bounds get tighter as K increases, such that, for instance, the Chernoff bound is around 1.5dB away from the exact PEP for $K = 0$, and this difference reduces to 0.7dB for $K = 2$ at PEP 10^{-6}. As occurred in the correlation case, as Fig. 5.5 depicts, the USTM scheme with the use of antenna selection operating on a Ricean channel exhibits the maximum attainable diversity order ($G_d = 4$) and significantly outperforms a system without antenna selection.

5.6 Summary

This chapter analyzed the performance of USTM and RAS over the spatially-correlated or Ricean fading channels. Two popular correlation models, exponential and constant models were considered. A good approximation to the CDF of a noncentral quadratic form in complex RV as a function of SNR was provided. Antenna selection was performed at the receiver, and the selection was based on the instantaneous received signal power. Our analysis was based on Chernoff bound. The simulations

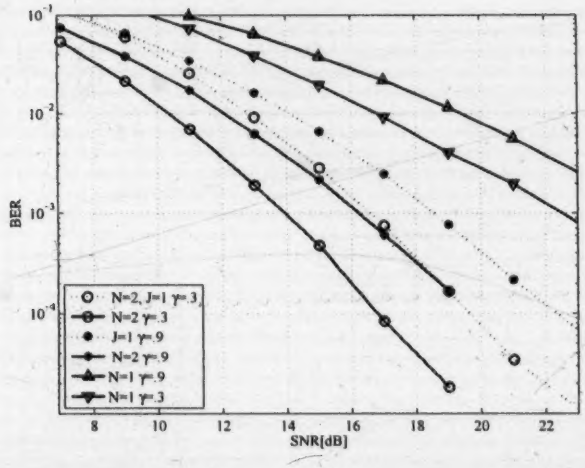

Figure 5.3: Performance comparison of parametric codes for the system with or without antenna selection and $M = 2$, $L = 16$ over spatially correlated channel

showed that although the antenna correlation degraded the coding gain of the system, the diversity order remained the same as that of a full-complex system as long as the unitary signals were full rank. The same held for the Ricean channel case with any K-factor. For a simple 2×2 differential USTM system with single receive antenna selection, the Chernoff bound expression was simplified and the simulation results for for both correlated and Ricean cases were presented.

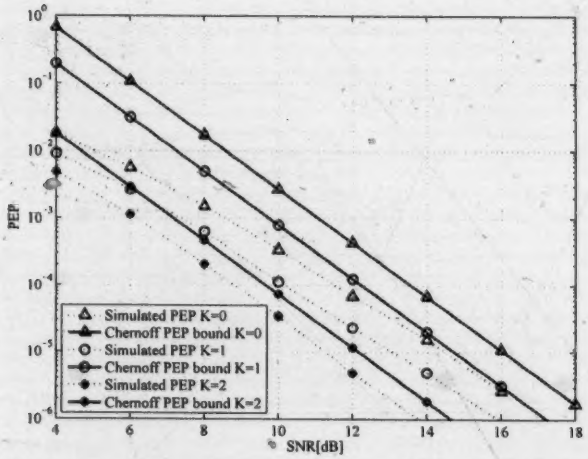

Figure 5.4: Comparison of the Chernoff bound and the simulated PEP for different K-factor $M = 2$, $N = 2$ $J = 1$

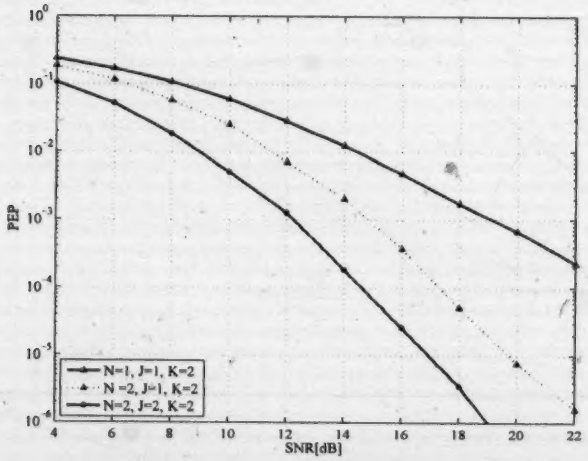

Figure 5.5: Performance comparison of parametric codes for the system with or without antenna selection and M=2, L=16 over a Ricean channel K=2

Chapter 6

Conclusion and Future Research

This thesis first provided a brief introduction to the MIMO systems and space time codes in Chapter 2. In Chapters 3, two new structures of unitary matrices were introduced, a closed-form approximation of union bound on SEP was derived, and genetic algorithms to find the optimal solution were presented. In Chapter 4, to construct the best unitary codebook for DUSTM over a transmit-correlated channel, a design measure was introduced that minimizes the Union bound. As expected, over the correlated channel, our proposed optimum codes showed a better performance than those of the previously existing codes. The performances of ML and differential(Non-ML) decoders were studied. The simulation results confirmed that both these decoders performed approximately the same at high SNR.

For future research, USTM and DUSTM may be exploited in cooperative networks to develop a cooperative diversity scheme which bypasses the need for CSI. In fact, the sources and relays in such a system form a distributed (virtual) antenna array to effect spatial diversity gains. Therefore, distributed versions of USTM and DUSTM should be designed for this scenario. To the best of our knowledge, only a few works (such as [58]) have recently addressed this issue; however, many important issues remain relatively unexplored and worthy of future research.

In Chapter 5, the performances of the USTM with single antenna selection was investigated for the spatially correlated channel, where the single antenna selection is performed at the receiver, and the selection is based on the instantaneous-received-signal power. To model the correlation between each pair of transmit antennas, two popular matrix models were used. Our analysis was extended for the

Ricean channel by providing a good approximation of the CDF of the noncentral quadratic form (QF) of the complex Gaussian RVs as a function of SNR. Our analysis as well as our simulations showed that the correlation degraded the coding gain of the system while the diversity order remained unaffected. Since the derived CDF expression for the non-central QF of Gaussian RV converged better than existing CDF expressions, that CDF expression may also have other applications. For instance, to calculate the BER of a differential or non-coherent decode-and-froward scheme, the distribution of a Gaussian QF is required [59].

Finally, this thesis considered only the case of single antenna selection. Performance analysis for USTM with multiple antenna selection is a possible future research topic.

Appendix A

Appendices

A.1 Proof of Theorem 5.3.2

A.2 Proof of Theorem 5.3.2

By Induction theorem, let $f(s) = \left(\prod_{i=1}^{M}[1+sr_i]^{-1}\right)$. For $k = 0$, it is clear that

$$f(s)\Big|_{s=-1} = C_0\rho^{-M} + o(\rho^{-M}), \tag{A.1}$$

where $C_0 = (-M/T)^M \det^{-1}(\mathbf{R}_T)$. Similarly, for $k = 1, 2$, we find

$$f'(s)\Big|_{s=-1} = \sum_{i=1}^{M} -r_i(1+r_is)^{-1}f(s)\Big|_{s=-1} = C_1\rho^{-M} + o(\rho^{-M}) \tag{A.2}$$

$$\begin{aligned} f''(s)\Big|_{s=-1} &= \sum_{i=1}^{M} r_i^2(1+r_is)^{-2}f(s)\Big|_{s=-1} + \sum_{i=1}^{M} -r_i(1+r_is)^{-1}f'(s)\Big|_{s=-1} \\ &= C_2\rho^{-M} + o(\rho^{-M}), \end{aligned} \tag{A.3}$$

where $C_1 = MC_0$, and $C_2 = M(M+1)C_0$. Assuming that for all $k < n$ $f^{(k)}(s)\big|_{s=-1} = C_k\rho^{-M} + o(\rho^{-M})$, we show that for $k = n$ the same relation is held. i.e. $f^{(n)}(s)\big|_{s=-1} = C_n\rho^{-M} + o(\rho^{-M})$. By using the same extension procedure used in (A.3), the nth derivative of $f(s)$ is expressed as a series of lower order derivatives:

$$f^{(n)}(s) = \beta_n \sum_{i=1}^{M} r_i^n(1+r_is)^{-n}f(s) + \cdots + \beta_1 \sum_{i=1}^{M} r_i(1+r_is)^{-1}f^{(n-1)}(s), \tag{A.4}$$

where $\beta_1, \ldots, \beta_n$ are independent of ρ and can be obtained from: $\beta_i = (-1)^i(n-1)!/(n-i)!$. In fact, presenting a general-closed form for C_k seems to be difficult; however for a small k, C_k is very easy to calculate.

A.3 Demonstration of Convergence Properties of Proposed Series and [1]

Due to the many application in statistics and communication theory, the CDF and PDF of quadratic forms have received much attention. Various series expansions and approximations have been developed [51] and [1]. Most of them except the power series in [1] are complicated and hard to use in practice. In order to obtain the most dominant term in the power series, we could rely on and adapt the numerical techniques presented in [1] for either the Ricean or correlated channel case. Although the obtained formulas for CDFs for both cases seem to be much more simplified than those we derived in our paper, the radius of convergence for these series totally depends on the value of y. We will make this point clear shortly. For comparison, we apply our case to the power series in [1], but first, we give a quick summary of the approach in [1]. Consider a simplified quadratic form $z = \mathbf{y}^H\mathbf{y}$, where $\mathbf{y}$ is a $T \times 1$ Gaussian random vector with mean $\overline{\mathbf{y}}$. The covariance matrix $\mathbf{R}$ is assumed to be full rank and to have a factorization $\mathbf{R} = \mathbf{U}\boldsymbol{\Sigma}\mathbf{U}^H$ where $\boldsymbol{\Sigma} = \text{diag}\{\sigma_1, \ldots, \sigma_T\}$, and $\mathbf{U}$ is a unitary matrix. Since $\mathbf{R}$ is assumed to be full rank (i.e., $\delta = 0$ c.f. [1]), the CDF function of z for $a \geq 0$ is given by [1]

$$F_z(a) = \sum_{k=0}^{\infty} c_k \frac{a^{T+k}}{(T+k)!}, \tag{A.5}$$

where

$$c_0 = \frac{1}{\det(\mathbf{R})} \exp\left(-\sum_{j=1}^{T} \frac{|b_j|^2}{\sigma_j^2}\right) \tag{A.6}$$

$$c_k = \frac{1}{k}\sum_{r=0}^{k-1} d_{k-r}c_r$$

$$d_k = (-1)^k \sum_{j=1}^{T}\left(\frac{1}{\sigma_j^k} - \frac{k|b_j|^2}{\sigma_j^{k+2}}\right). \tag{A.7}$$

Moreover, vector $\mathbf{b}$ is defined as $\mathbf{b} = [b_1, \ldots, b_T]^{\mathsf{T}} = \boldsymbol{\Sigma}^{\frac{1}{2}}\mathbf{U}^H\overline{\mathbf{y}}$. By carefully setting up matrix $\mathbf{R}$ and vector $\overline{\mathbf{y}}$ from equations (5.34) and (5.36), respectively, we can evaluate the CDF for the Ricean fading scenario. This formula is applied to the correlated channel as well considering that $\overline{\mathbf{y}} = \mathbf{0}$. As mentioned earlier, our ultimate aim for deriving the CDF function is to determine the first term in (A.5) with respect to ρ. The exponential term in the right side of (A.6) can be rewritten as

$$\sum_{j=1}^{T} \frac{|b_j|^2}{\sigma_j^2} = \mathbf{b}^H\boldsymbol{\Sigma}^{-2}\mathbf{b} = \overline{\mathbf{y}}^H\mathbf{R}_l^{-1}\overline{\mathbf{y}} = \frac{x}{1+x}K\|\overline{\mathbf{h}}\|_F^2 \to K\|\overline{\mathbf{h}}\|_F^2, \qquad x \to \infty \tag{A.8}$$

where $x = \frac{\rho T}{M(K+1)}$. Therefore, (A.6) reduces to

$$c_0 = x^{-M}e^{-K\|\overline{\mathbf{h}}\|_F^2} + o(x^{-M}) \tag{A.9}$$

Notice that factor ρ^{-M} has appeared in (A.9), and that since the coefficient c_k is calculated recursively from $c_0, \ldots, c_{k-1}$, only the constant term with respect to ρ is taken into account in d_k (A.7); i.e.,

$$\begin{aligned} d_k &= (-1)^k[\mathrm{tr}(\boldsymbol{\Sigma}^{-k}) - k\mathbf{b}^H\boldsymbol{\Sigma}^{-(k+2)}\mathbf{b}] \\ &= (-1)^k[T - M + M(1+x)^{-k} - k\overline{\mathbf{y}}^H\mathbf{R}_l^{-(k+1)}\overline{\mathbf{y}}] \\ &\overset{(a)}{=} (-1)^k[T - M + M(1+x)^{-k} - kx(1+x)^{-(k+1)}K\|\overline{\mathbf{h}}\|_F^2] \\ &= (-1)^k(T-M) + o(x^{-k}) \quad \forall k > 1, \end{aligned} \tag{A.10}$$

where (a) results from the following lemma:

Lemma 1 *For the covariance matrix of (5.34) and positive integer m, we have*

$$\mathbf{R}^{-m} = \mathbf{I}_T + \boldsymbol{\Phi}_l\boldsymbol{\Phi}_l^H[(1+x)^{-m} - 1)].$$

Proof A.3.1 *Using the binomial expansion, we obtain*

$$\begin{aligned} \mathbf{R}^{-m} &= (\mathbf{I}_T - \frac{x}{1+x}\boldsymbol{\Phi}_l\boldsymbol{\Phi}_l^H)^m = \mathbf{I}_T - \boldsymbol{\Phi}_l\boldsymbol{\Phi}_l^H + \sum_{p=0}^{m}\binom{m}{p}\boldsymbol{\Phi}_l\boldsymbol{\Phi}_l^H(\frac{-x}{1+x})^p \\ &= \mathbf{I}_T + \boldsymbol{\Phi}_l\boldsymbol{\Phi}_l^H\left[(1 - \frac{x}{1+x})^m - 1\right], \end{aligned} \tag{A.11}$$

which completes the proof.

The first term in the power series of CDF with respect to ρ is stated as

$$F_z(a) = \rho^{-M} \sum_{k=0}^{\infty} \hat{c}_k \frac{a^{K+T}}{(K+T)!} + o(\rho^{-M}), \tag{A.12}$$

where

$$\begin{aligned} \hat{c}_0 &= \left[\frac{M(K+1)}{T}\right]^M e^{-K\|\bar{\mathbf{h}}\|_F^2} \\ \hat{d}_k &= (-1)^k (T-M) \\ \hat{c}_k &= \frac{1}{k} \sum_{r=0}^{k-1} \hat{d}_{k-r} \hat{c}_r. \end{aligned} \tag{A.13}$$

The formula in (A.12) is much more simplified than (5.47). Hence, one may ask why we did not use this formula in (5.49) to compute the Chernoff bound. Although this formula seems to be less complex than (5.4.2), formula (A.12), on the other hand, shows significantly poorer convergence over wider range of a. To clarify the difference in the convergence behavior, we compare our obtained CDF formulas and the CDF power series in [1] in terms of the mean square error (MSE[1]) for both the correlated and Ricean channel cases. Note that (5.4.2) has been derived for the Ricean channel case; however, with a small change, it can be applied to the correlation channel case as well. For 180 uniformly spaced data points in the interval $2 \leq a \leq 20$, Fig. A.1 shows that the MSE of $F_z(a)$ as a function of the number of terms adds up in (5.4.2). As we observe for a particular MSE, (5.4.2) needs significantly more terms than formula (5.33), which is actually independent of the number of terms. The convergence behavior of (A.12) even becomes worse at a higher value of a, such that if we insert it into the P_{CB} expression in (5.38), computing P_{CB} becomes numerically impossible . Because we are required to take the integral of $F_z(a)$ over all values of a in (5.38) while the radius of convergence of the power series is highly dependent on a. We therefore resort to our formulas for calculating Chernoff bounds.

[1] See [1] for the definition of MSE

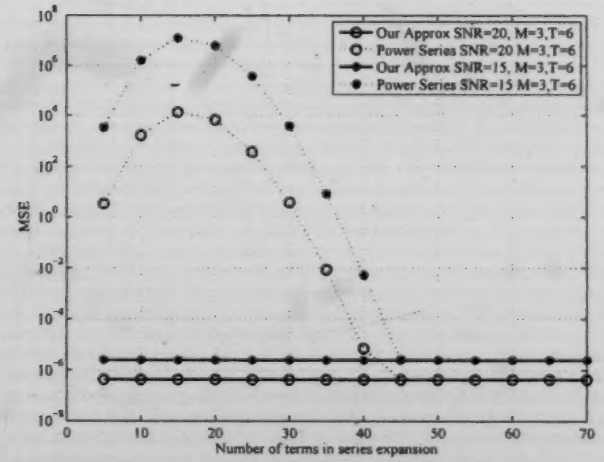

Figure A.1: Comparison of the convergence properties of the power series expansion and our formula for $F_z(a)$ assuming constant correlation matrix with $\gamma = 0.5$

Bibliography

[1] R. U. Nabar, H. Bolcskei, and A. J. Paulraj, "Diversity and outage performance in space-time block coded Ricean MIMO channels," *IEEE Trans. Wireless Commun.*, vol. 4, no. 5, pp. 2519–2532, Sept. 2005.

[2] B. Hochwald and W. Sweldens, "Differential unitary space-time modulation," *IEEE Trans. Commun.*, vol. 48, no. 12, pp. 2041 – 2052, Dec. 2000.

[3] I. Telatar and D. Tse, "Capacity and mutual information of wideband multipath fading channels," *IEEE Trans. Inform. Theory*, vol. 46, no. 4, pp. 1384 – 1400, July 2000.

[4] G. Foschini and M. Gans, "On limits of wireless communications in a fading environment when using multiple antennas," *Wirel. Pers. Commun. (Netherlands)*, vol. 6, no. 3, pp. 311 – 335, Mar. 1998.

[5] T. L. Marzetta and B. M. Hochwald, "Capacity of a mobile multiple-antenna communication link in Rayleigh flat fading," *IEEE Trans. Inform. Theory*, vol. 45, pp. 139–157, Jan. 1999.

[6] B. Hochwald and T. Marzetta, "Unitary space-time modulation for multiple-antenna communications in Rayleigh flat fading," *IEEE Trans. Inform. Theory*, vol. 46, no. 2, pp. 543 – 564, Mar. 2000.

[7] B. Hochwald, T. Marzetta, T. Richardson, W. Sweldens, and R. Urbanke, "Systematic design of unitary space-time constellations," *IEEE Trans. Inform. Theory*, vol. 46, no. 6, pp. 1962 – 1973, Sept. 2000.

[8] H. Zhang, H. Dai, Q. Zhou, and B. L. Hughes, "On the diversity order of spatial multiplexing systems with transmit antenna selection: A geometrical

approach," *IEEE Transactions on Information Theory*, vol. 52, no. 12, pp. 5297–5311, Dec. 2006.

[9] V. Tarokh, N. Seshadri, and A. R. Calderbank, "Space-time codes for high data rate wireless communication: Performance analysis and code construction," *IEEE Trans. Inform. Theory*, vol. 44, pp. 744–765, Mar. 1998.

[10] S. Alamouti, "A simple transmit diversity technique for wireless communications," *IEEE J. Select. Areas Commun.*, vol. 16, pp. 1451 – 1458, Oct. 1998.

[11] R. N. A. Paulraj and D. Gore, *Introduction to Space-Time Wireless Communications*, 1st ed. Cambridge University Press, 2003.

[12] X. Cai and G. Giannakis, "Differential space-time modulation with eigenbeamforming for correlated MIMO fading channels," *IEEE Trans. Signal Processing*, vol. 54, no. 4, pp. 1279–1288, 2006.

[13] B. Holter and G. Oien, "On the amount of fading in MIMO diversity systems," *IEEE Trans. Wireless Commun.*, vol. 4, no. 5, pp. 2498–2507, 2005.

[14] M.-S. Alouini, A. Abdi, and M. Kaveh, "Sum of Gamma variates and performance of wireless communication systems over Nakagami-fading channels," *IEEE Trans. Veh. Technol.*, vol. 50, pp. 1471 –1480, Nov. 2001.

[15] C.-N. Chuah, D. Tse, J. Kahn, and R. Valenzuela, "Capacity scaling in MIMO wireless systems under correlated fading," *IEEE Trans. Inform. Theory*, vol. 48, no. 3, pp. 637–650, 2002.

[16] C. Tepedelenlioglu, A. Abdi, and G. B. Giannakis, "The Ricean K factor: estimation and performance analysis," *IEEE Trans. Commun.*, vol. 2, no. 4, pp. 799–810, July 2003.

[17] B. Hughes, "Differential space-time modulation," *IEEE Trans. Inform. Theory*, vol. 46, no. 7, pp. 2567–2578, 2000.

[18] I. Bahceci, T. Duman, and Y. Altunbasak, "Antenna selection for multiple-antenna transmission systems: performance analysis and code construction,"

in *Proc. IEEE Int. Symp. on Infor. Theory (ISIT)*, Yokohama, Japan, 2003, pp. 93 –.

[19] D. A. Gore and A. J. Paulraj, "MIMO antenna subset selection with space-time coding," *IEEE Trans. Signal Processing*, vol. 50, no. 10, pp. 2580–2588, Oct. 2002.

[20] A. F. Molisch, M. Z. Win, and J. H. Winters, "Capacity of MIMO systems with antenna selection," in *Proc. IEEE Int. Conf. Communications (ICC)*, vol. 2, Helsinki, Finland, 2001, pp. 570–574.

[21] A. Gorokhov, "Antenna selection algorithms for MEA transmission systems," *Proc. IEEE Int. Conf. Acoustics, Speech, and Signal Processing (ICASSP)*, vol. 3, 2002.

[22] A. Ghrayeb and T. Duman, "Performance analysis of MIMO systems with antenna selection over quasi-static fading channels," in *Proc. IEEE Int. Symp. on Infor. Theory (ISIT)*, Lausanne, Switzerland, 2002, pp. 333 –.

[23] I. Bahceci, T. Duman, and Y. Altunbasak, "Antenna selection for multiple-antenna transmission systems: performance analysis and code construction," *IEEE Trans. Inform. Theory*, vol. 49, no. 10, pp. 2669 – 2681, Oct. 2003.

[24] Q. Ma and C. Tepedelenlioglu, "Antenna selection for unitary space-time modulation," *IEEE Trans. Inform. Theory*, vol. 51, no. 10, pp. 3620–3631, Oct. 2005.

[25] G. D. Golden, G. J. Foschini, R. A.Valenzuela, and P. W.Wolniansky, "Detection algorithm and initial laboratory results using the V-BLAST space-time communication architecture," *IEE Elect. Lett.*, vol. 35, pp. 14–15, Jan. 1999.

[26] G. Foschini, G. Golden, R. Valenzuela, and P. Wolniansky, "Simplified processing for high spectral efficiency wireless communication employing multi-element arrays," *IEEE J. Select. Areas Commun.*, vol. 17, no. 11, pp. 1841–1852, 1999.

[27] B. Hassibi, "An efficient square-root algorithm for BLAST," in *Proc. IEEE Int. Conf. Acoustics, Speech, and Signal Processing (ICASSP)*, vol. 2, Istanbul, 2000.

[28] T. Xiaofeng, C. Elena, Y. Zhuizhuan, Q. Haiyan, and Z. Ping, "New detection algorithm of V-BLAST space-time code," in *Vehicular Technology Conference, 2001. VTC 2001 Fall. IEEE VTS 54th*, vol. 4, Atlantic City, NJ, 2001, pp. 2421–2423.

[29] V. Tarokh, H. Jafarkhani, and A. Calderbank, "Space-time block codes from orthogonal designs," *IEEE Trans. Inform. Theory*, vol. 45, no. 5, pp. 1456 – 1467, July 1999.

[30] G. J. Foschini, "Layered space-time architecture for wireless communication in a fading environment when using multi-element antennas," *Bell Labs Tech. J.*,, vol. 1, pp. 41–59, 1996.

[31] M. O. Damen, A. Chkeif, and J. C. Belfiore, "Lattice codes decoder for space-time codes," *IEEE Commun. Lett.*, vol. 4, pp. 161–163, May 2000.

[32] M. O. Damen, K. Abed-Meraim, M. S. Lemdani, "Further results on the sphere decoder," *Proc. IEEE Int. Symp. on Infor. Theory (ISIT)*, p. 33, June 2001.

[33] T. P. Soh, C. S. Ng, and P. Y. Kam, "Improved signal constellations for differential unitary space-time modulations with more than two transmit antennas," *IEEE Commun. Lett.*, vol. 9, no. 1, pp. 7 – 9, 2005.

[34] C. Shan, A. Nallanathan, and P. Y. Kam, "A new class of signal constellations for differential unitary space-time modulation (DUSTM)," *IEEE Commun. Lett.*, vol. 8, no. 1, pp. 1 – 3, 2004.

[35] J. Wang, M. Simon, and K. Yao, "On the optimum design of differential unitary space-time modulation," *IEEE Global Telecommn. Conf. (GLOBECOM)*, vol. 4, pp. 1968 – 72, 2003.

[36] P. Dita, "Factorization of unitary matrix," *Journal of PhysicsA :Mathematic and General*, vol. 36, pp. 2781 – 2789, Mar. 2003.

[37] X. Liang and X. Xia, "Unitary signal constellations for differential spacetime modulation with two transmit antennas: Parametric codes, optimal designs, and bounds," *IEEE Trans. Inform. Theory*, vol. 48, pp. 2291 – 2322, Aug. 2002.

[38] M. Abramowitz and I. A. Stegun, *Handbook of Mathematical Functions with Formulas, Graphs, and Mathematical Tables*. New York: Dover, 1972.

[39] Z. Michalewicz, *Genetic Algorithms + Data Structures = Evolution Programs, 3rd ed.* Berlin ; New York : Springer-Verlag, c1992., 1992.

[40] J. Holland, *Adaptation in Natural and Artificial Systems*. University of Michigan Press, 1975.

[41] Z. Michalewicz, *Genetic Algorithms + Data Structures = Evolution Programs, 3rd ed.* Berlin ; New York : Springer-Verlag, c1992., 1992.

[42] D. Liu, Q. Zhang, and Q. Chen, "Structures and performance of noncoherent receivers for unitary space-time modulation on correlated fast-fading channels," *IEEE Trans. Veh. Technol.*, vol. 53, no. 4, pp. 1116–1125, 2004.

[43] D.-S. Shiu, G. Foschini, M. Gans, and J. Kahn, "Fading correlation and its effect on the capacity of multi-element antenna systems," *IEEE Trans. Commun.*, vol. 48, no. 3, pp. 502–513, 2000.

[44] H. Wang, Z. Li, and J. Lilleberg, "Equalized parallel interference cancellation for MIMO MC-CDMA downlink transmissions," in *IEEE Int. Symposium on Personal, Indoor and Mobile Radio Commun. (PIMRC)*, vol. 2, Beijing, China, 2003, pp. 1250 – 1254.

[45] M. Hajiaghayi and C. Tellambura, "Unitary signal constellations for differential space-time modulation," *IEEE Commun. Lett.*, vol. 11, no. 1, pp. 25–27, Jan. 2007.

[46] J. Heath, R.W., S. Sandhu, and A. Paulraj, "Antenna selection for spatial multiplexing systems with linear receivers," *IEEE Commun. Lett.*, vol. 5, no. 4, pp. 142 – 144, Apr. 2001.

[47] A. Gorokhov, D. Gore, and A. Paulraj, "Performance bounds for antenna selection in MIMO systems," in *Proc. IEEE Int. Conf. Communications (ICC)*, vol. 5, Anchorage, AK, USA, 2003, pp. 3021 – 3025.

[48] J. Heath, R. W. and D. J. Love, "Multimode antenna selection for spatial multiplexing systems with linear receivers," *IEEE Trans. Signal Processing*, vol. 53, pp. 3042–3056, Aug. 2005.

[49] D. Gore and A. Paulraj, "Space-time block coding with optimal antenna selection," in *Proc. IEEE Int. Conf. Acoustics, Speech, and Signal Processing (ICASSP)*, vol. 4, Salt Lake City, UT, USA, 2001, pp. 2441 – 2444.

[50] S. Jafar, S. Vishwanath, and A. Goldsmith, "Channel capacity and beamforming for multiple transmit and receive antennas with covariance feedback," in *Proc. IEEE Int. Conf. Communications (ICC)*, vol. 7, Helsinki, 2001, pp. 2266–2270.

[51] D. Raphaeli, "Distribution of noncentral indefinite quadratic forms in complex normal variables," *IEEE Trans. Inform. Theory*, vol. 42, no. 3, pp. 1002–1007, May 1996.

[52] M. Hasna, M.-S. Alouini, and M. Simon, "Effect of fading correlation on the outage probability of cellular mobile radio systems," in *Proc. IEEE Vehicular Technology Conf. (VTC)*, vol. 3, Atlantic City, NJ, USA, 2001, pp. 1794 – 1798.

[53] H. A. David, *Order statistics*, 2nd ed. New York : Wiley, 1981.

[54] M. Schwartz, W. R. Bennett, and S. Stein, *Communication Systems and Techniques*. New York: McGraw-Hill, 1966.

[55] R. A. Horn and C. R. Johnson, *Matrix Analysis*. Cambridge, U.K.: Cambridge Univ. Press, 1985.

[56] Z. Wang and G. B. Giannakis, "A simple and general parameterization quantifying performance in fading channels," *IEEE Trans. Commun.*, vol. 51, no. 8, pp. 1389–1398, Aug. 2003.

[57] M. Hajiaghayi, M. Ramezani, and C. Tellambura, "Antenna selection for unitary space-time modulation over Correlated and Ricean channels," *to be sumbitted to IEEE Trans. Wireless Commun.*, Sept. 2007 (Also see www.ece.ualberta.ca/ mahdih/paper3.pdf).

[58] T. Wang, Y. Yao, and G. B. Giannakis, "Non-coherent distributed space-time processing for multiuser cooperative transmissions," *IEEE Trans. Wireless Commun.*, vol. 5, no. 12, pp. 3339–3343, Dec. 2006.

[59] N. Shah and H. Li, "Distribution of quadratic form in gaussian mixture variables and an application in relay networks," in *IEEE Workshop on Signal Processing advances in Wireless Commun.*, June 2005, pp. 490–494.